FROM RESEARCH TO INDUSTRY

cea

mircen

MOLECULAR IMAGING RESEARCH CENTER

GPU BASED MODELING PIPELINE TO EXTRACT BRAIN CELL MORPHOLOGY FROM IN VIVO DIFFUSION-WEIGHTED MR SPECTROSCOPY DATA

Palombo M., Ligneul C., Najac C., Le Douce J., Flament J., Escartine C., Hantraye P., Brouillet E., Bonvento G., Valette J.

CEA/DSV/I²BM, MIRCEN, FONTENAY-AUX-ROSES, FRANCE

OUTLINE

- Introduction and Rationale;
- Application 1: Brain cell's morphology extraction;
- Application 2: finer cell's morphology characterization
- Future Perspectives: applications to pathology

INTRODUCTION

MOLECULAR DIFFUSION MEASURED BY DIFFUSION-WEIGHTED MR

Possibility to investigate the apparent diffusion of endogenous molecules

Diffusion-weighted MRI: water

Ischemic stroke Fiber tracking

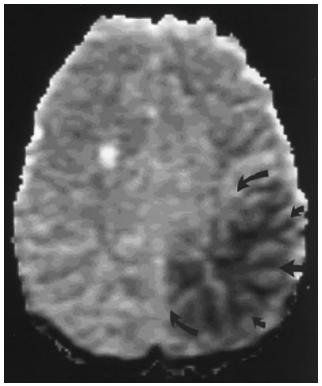

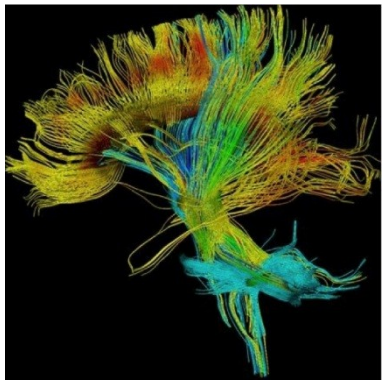

High sensitivity

Good spatial resolution (1 mm^3)

Non invasive

INTRODUCTION

MOLECULAR DIFFUSION MEASURED BY DIFFUSION-WEIGHTED MR

Possibility to investigate the apparent diffusion of endogenous molecules

Diffusion-weighted MRI: water

Ischemic stroke Fiber tracking

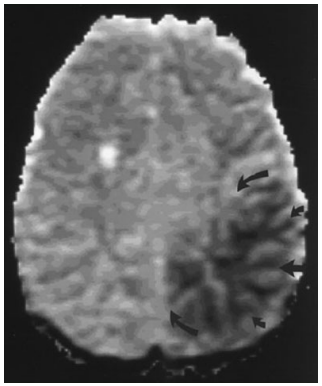

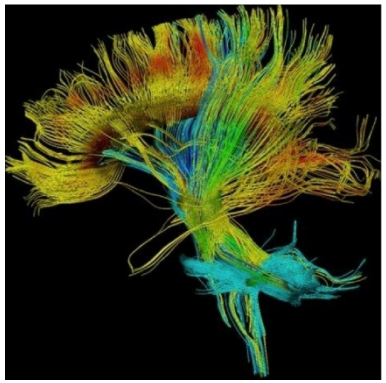

High sensitivity

Good spatial resolution (1 mm³)

Non invasive

Histological Microscopy

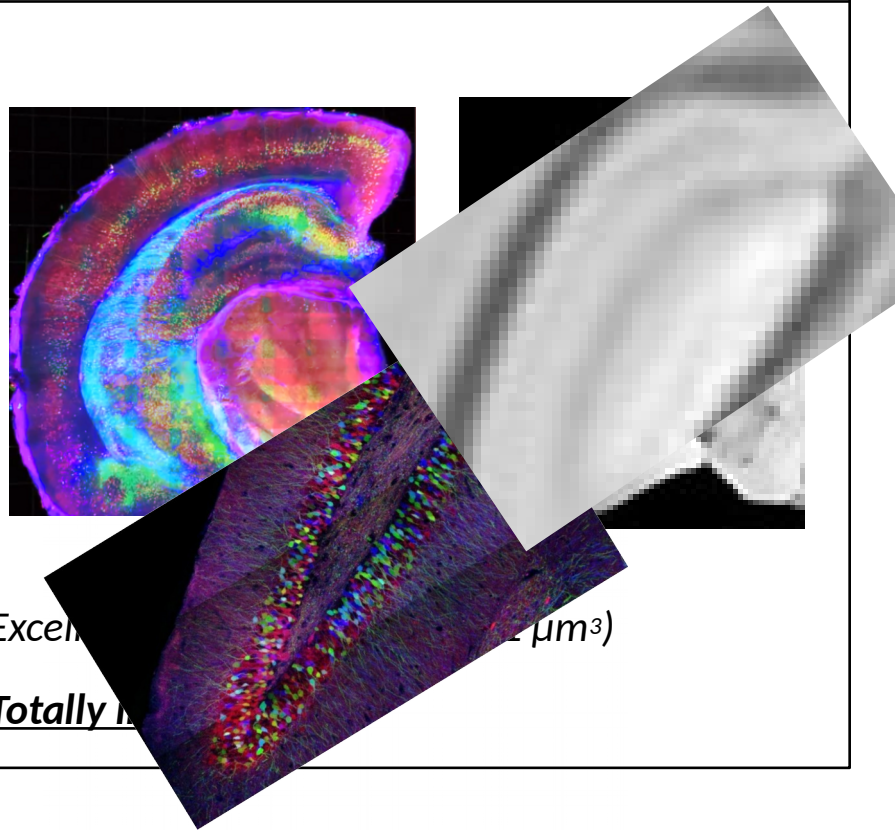

Excel *µm³)*

Totally i

INTRODUCTION

MOLECULAR DIFFUSION MEASURED BY DIFFUSION-WEIGHTED MR

Possibility to investigate the apparent diffusion of endogenous molecules

Diffusion-weighted MRI: water

Ischemic stroke Fiber tracking

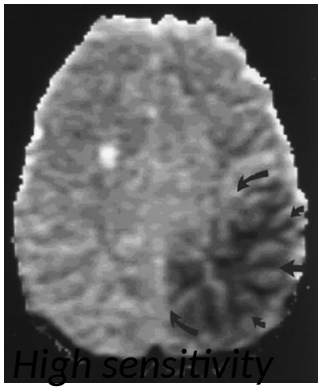

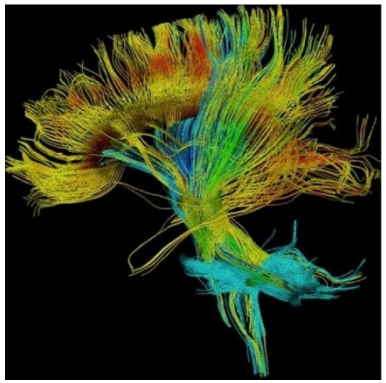

High sensitivity

Good spatial resolution (1 mm³)

Non invasive

Histological Microscopy

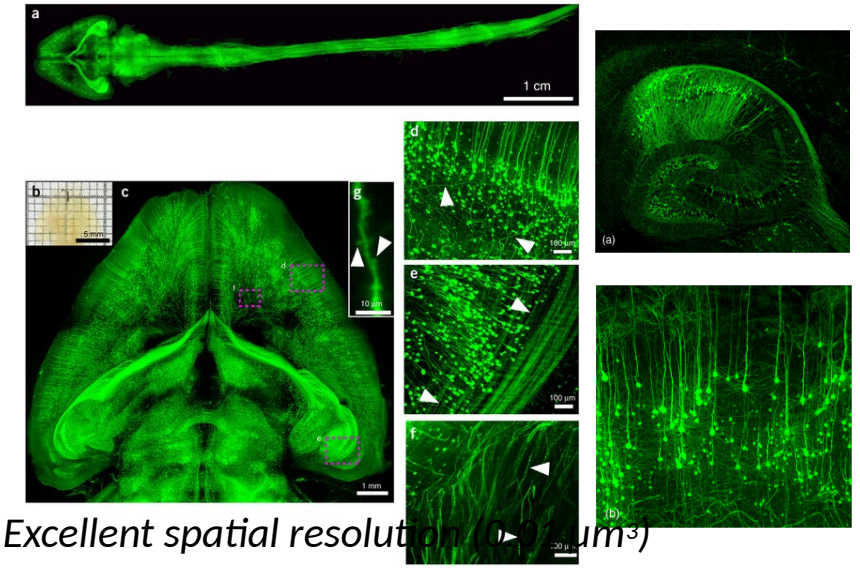

Excellent spatial resolution (0.01 µm³)

Totally invasive

INTRODUCTION

MOLECULAR DIFFUSION MEASURED BY DIFFUSION-WEIGHTED MR

Possibility to investigate the apparent diffusion of endogenous molecules

Diffusion-weighted MRI: water

Ischemic stroke Fiber tracking

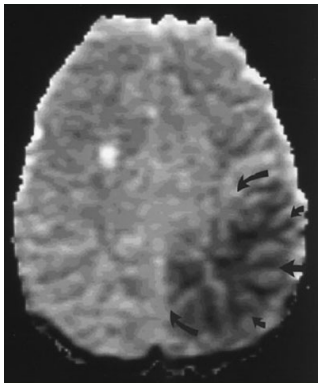

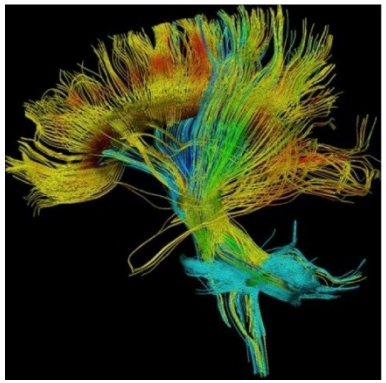

High sensitivity

But: Diffusion of water = ***no specific*** (extra + intracellular space, crosses membranes)

INTRODUCTION

AIM AND RATIONALE

Brain intracellular metabolites are primarily localized and diffuse in cell fibers rather than in cell bodies[1-4]

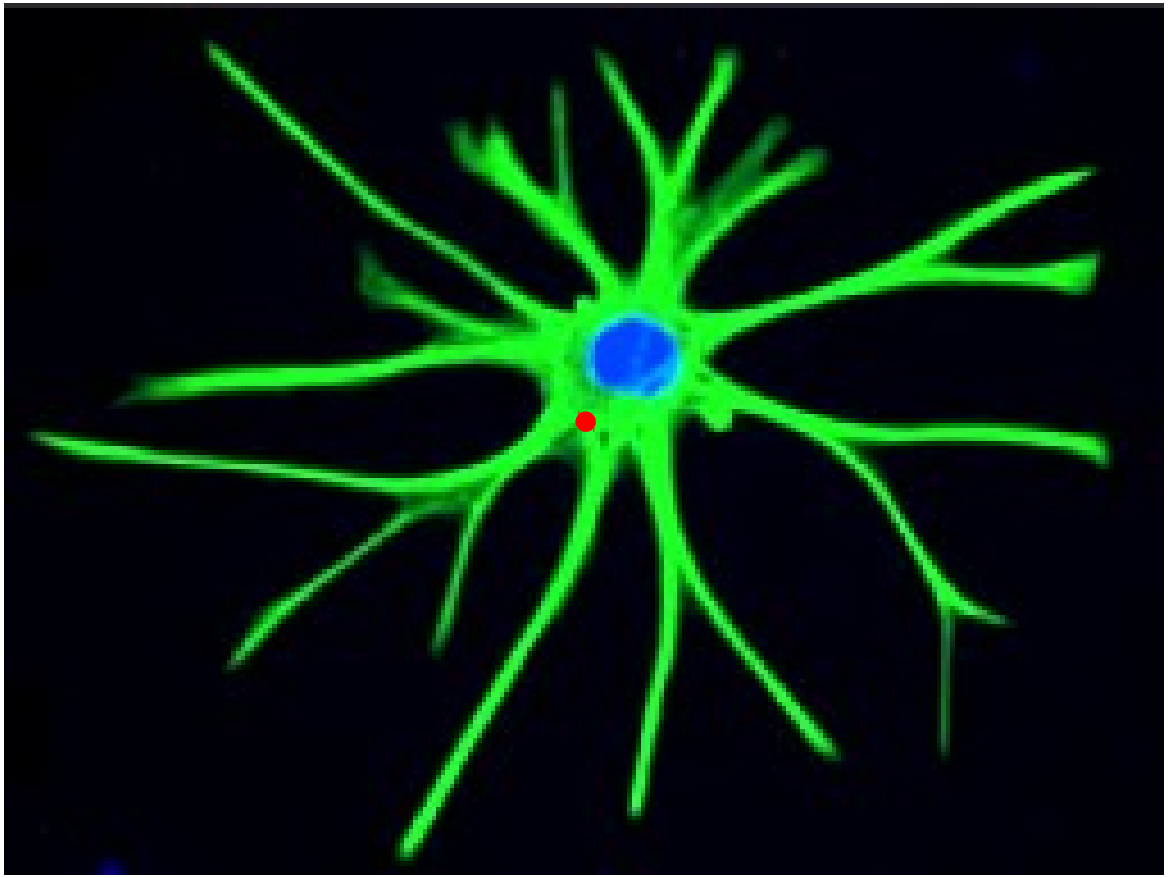

→ ***Interpretation*** and ***modeling*** of ***metabolite diffusion*** primarily based on ***cell geometry***

(1) Marchadour C et al. *Journal of Cerebral Blood Flow & Metabolism* (2012) **32 (12)**: 2153-2160;

(2) Najac C et al. *Neuroimage* (2014) **90**: 374-380;

(3) Najac C et al. *Brain Structure and Function* (2014) **221 (3)**: 1245-1254

(4) Ligneul C et al. *Magnetic Resonance in Medicine* (2016): **DOI: 10.1002/mrm.26217**

INTRODUCTION

AIM AND RATIONALE

Diffusion Weighted NMR

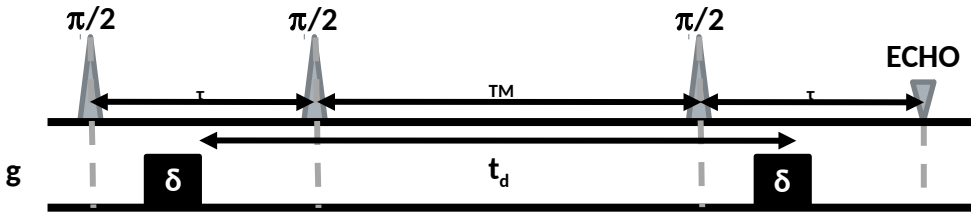

$$\rightarrow b = q^2 t_d \approx g^2 t_d$$

INTRODUCTION

AIM AND RATIONALE

Diffusion Weighted NMR

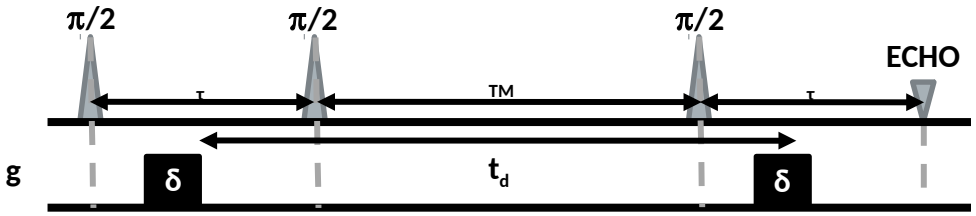

→ **b = $q^2 t_d \approx g^2 t_d$**

→ **S(b) ≈ exp[-b ADC(t_d)];** **ADC=<r(t_d)^2>/d t_d**

$$d\phi_j(t) = \gamma g(t) \cdot x_j(t) \Delta t$$

$$\phi_j = \sum_{t=0}^{t_{seq}} d\phi_j(t)$$

$$S = \left| \frac{1}{N} \sum_{j=1}^{N} e^{i\phi_j} \right|$$

$$ADC = - \frac{\ln(S / S_0)}{b}$$

$$b = \gamma^2 \int_0^{t_{seq}} dt \left[\int_0^t \vec{g}(t')\, dt' \right]^2$$

LONG DIFFUSION TIME EXPERIMENTS AND MODELING

METHODS

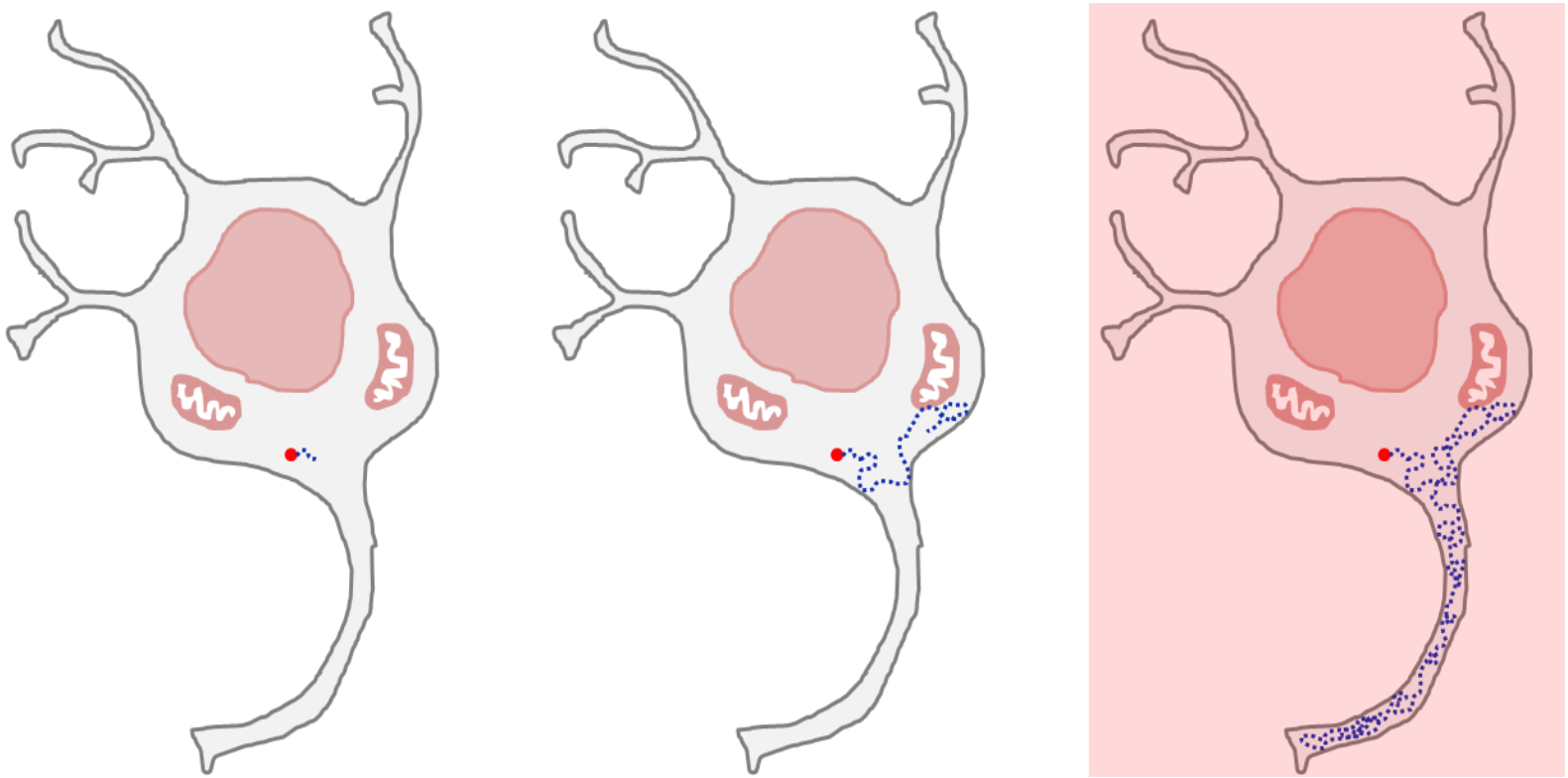

Diffusion time T_d	0.1 ms	1 ms	10 ms	100 ms	1 000 ms	10 000 ms
Distance traveled Δx	0.3 µm	1 µm	2 µm	5 µm	15 µm	50 µm
Parameters affecting apparent diffusion	*Intracellular viscosity*	*Fiber diameter (axons, dendrites…)* *Organelles*			*Cell size* *Long-range structural features*	

METHODS

MODELING

Astrocyte Neuron

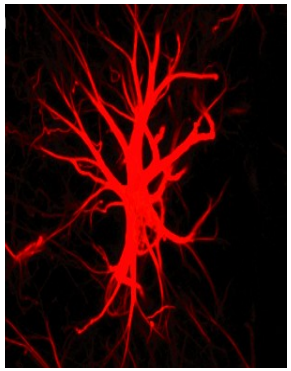

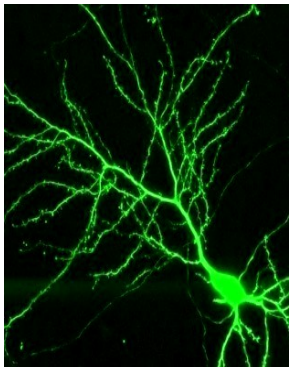

GFAP eGFP

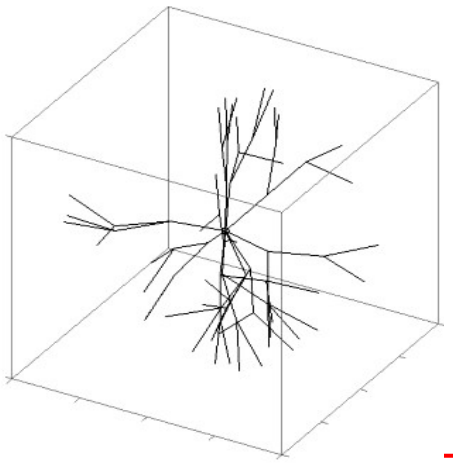

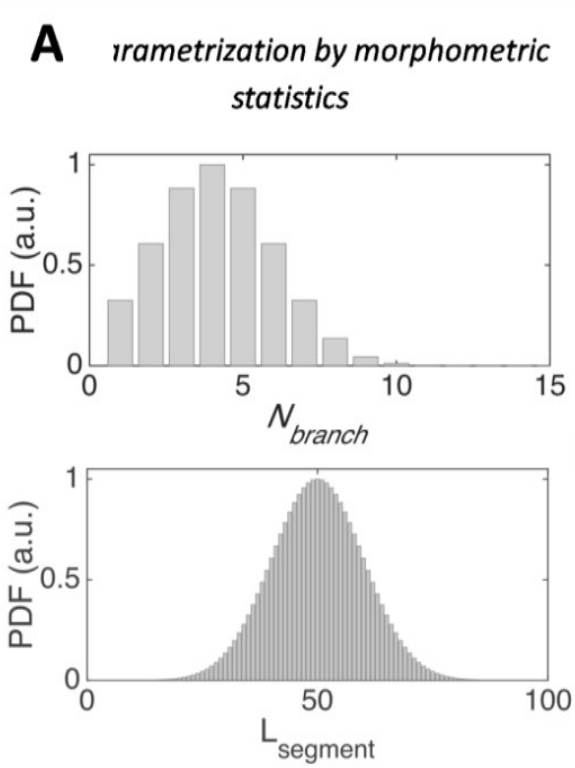

5 model parameters

D_{intra} = effective medium diffusivity (organelles and macromolecular crowding, spines, cytoplasm viscosity, etc…)

$L_{segment}$, N_{branch} = long-range topological characteristics

$SD_{Lsegment}$, $SD_{Nbranch}$ = metabolites compartments complexity and heterogeneity.

Palombo M. et al. *PNAS* (2016); **113**(*24*), 6671-6676

METHODS

SIMULATION-FITTING PIPELINE

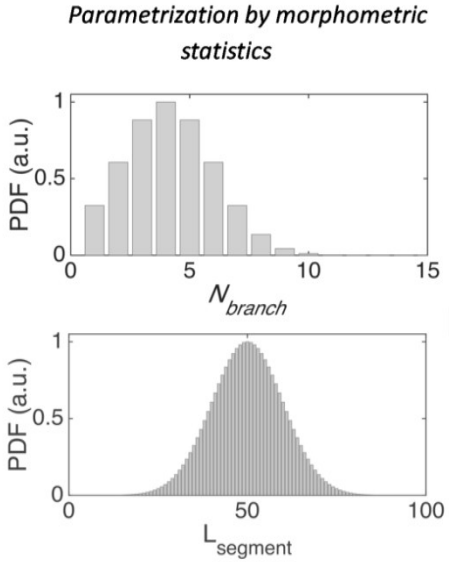

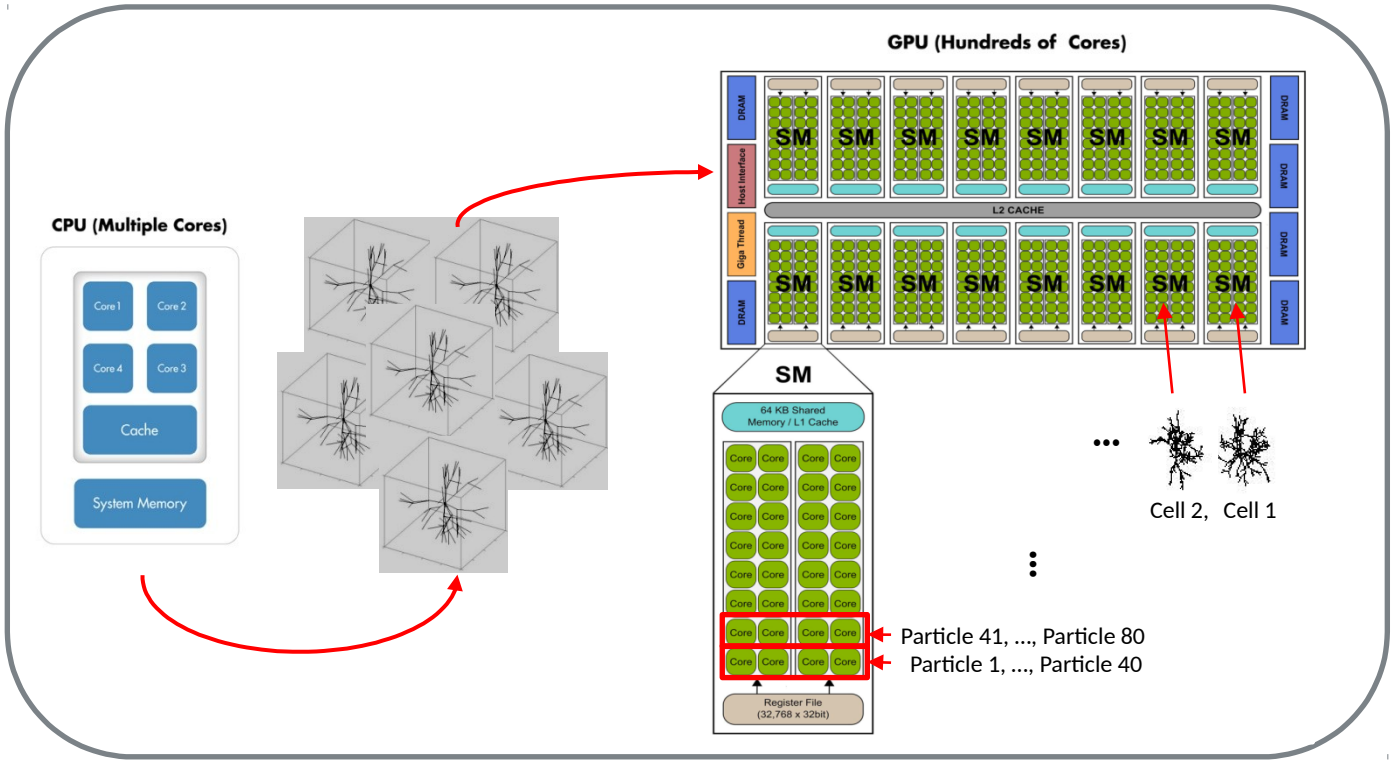

Palombo M. et al. *PNAS* (2016); **113**(*24*), 6671-6676

METHODS

MODELING

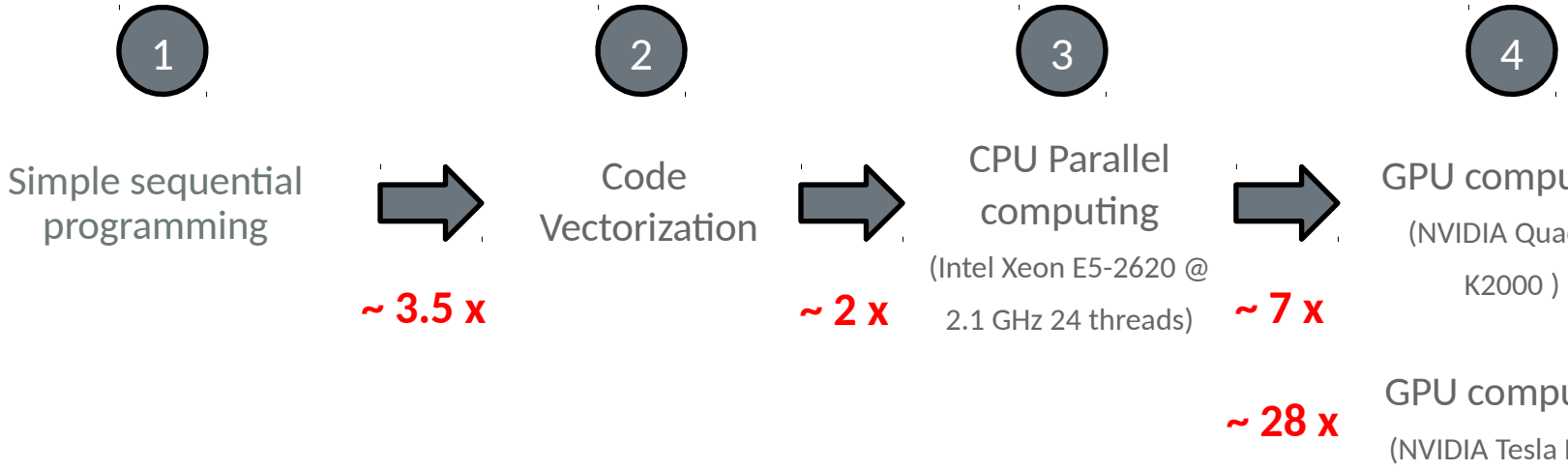

N particles = 10^3 ; N time step = 10^4 ; System replication = 50; Fitting iteration = 200 x 3;

Total iterations = ~ 10^{11}

	1	2	3	4
Fitting free diffusion data	**~ 17.5 minute**	**~ 5 minute**	**~ 3 minute**	**~ 0.1 minute**
Fitting restricted diffusion data	**~ 40 minute**	**~ 12 minute**	**~ 6 minute**	**~ 0.8 minute**

RESULTS

FITTING STABILITY TO EXPERIMENTAL NOISE

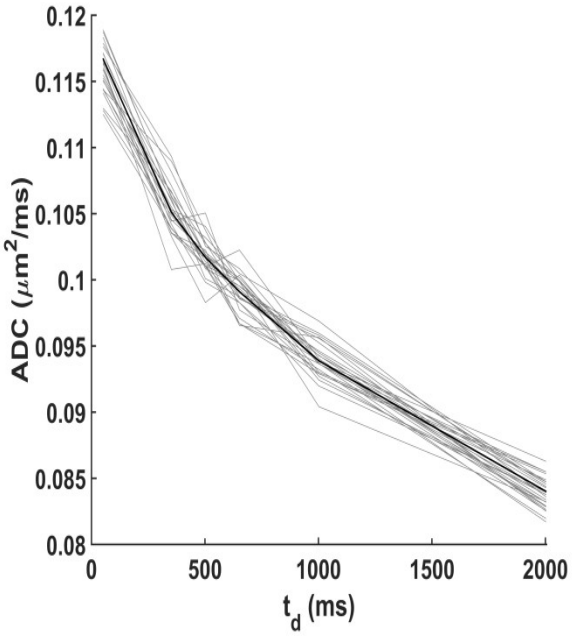

250 Monte-Carlo trials

Gaussian noise (15% relative SD) added to a reference simulated ADC(t_d) curve

Combined Parallel Tempering and Levenberg-Marquardt[$]

Unsupervised parameters initialization: refined grid-searching algorithm based on Parallel Tempering

Quick convergence to the optimal solution: Levenberg-Marquardt algorithm

Simulation-Fitting pipeline

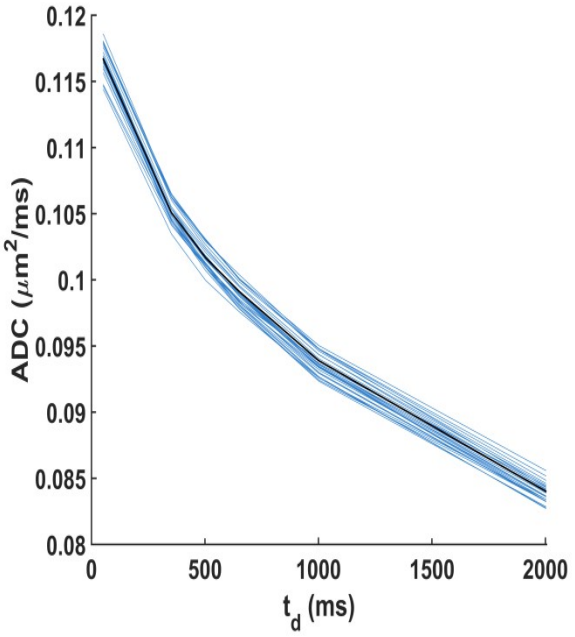

250 sets of fitted morphological parameters

$ Palombo M. et al. *Proceedings of the 23rd ISMRM Annual Meeting 2015*; ***Abstract # 2982***

RESULTS

FITTING STABILITY TO EXPERIMENTAL NOISE

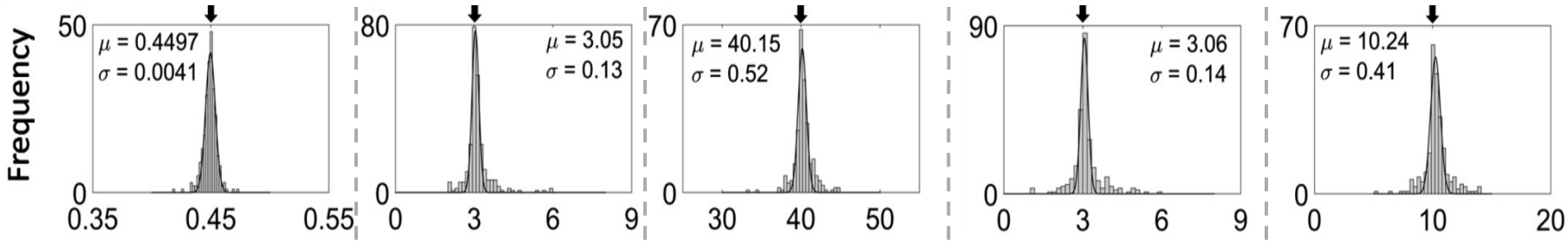

	D_{intra} ($\mu m^2/ms$)	N_{branch}	$L_{segment}$ (μm)	$SD_{Nbranch}$	$SD_{Lsegment}$ (μm)
Bias (%) $\mu/\mu_{true} - 1$	**-0.46**	**1.7**	**0.38**	**2.0**	**2.4**
CV (%) σ/μ_{true}	**0.91**	**4.3**	**1.3**	**4.7**	**4.1**

→ Fitting pipeline ***very stable*** (Bias and CV < 5%) ***with respect to experimental noise***

Palombo M. et al. *PNAS* (2016); **113**(*24*), 6671-6676

RESULTS

LONG DIFFUSION TIME EXPERIMENTS AND MODELING

Macaque

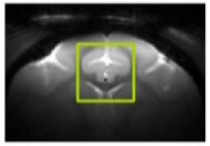

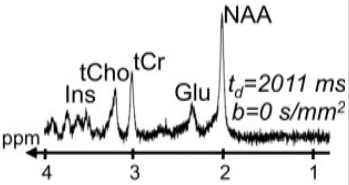

@ 7 T

Mouse

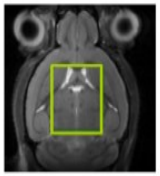

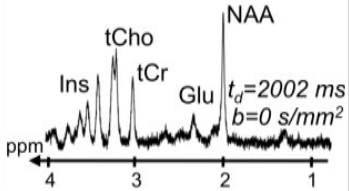

@ 11.7 T

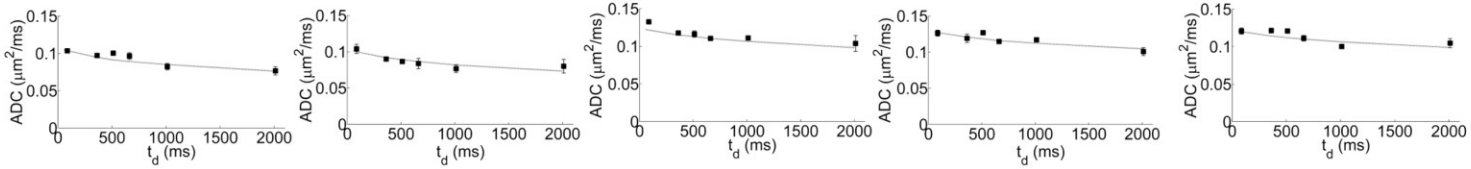

Ins **tCho** **tCr** **Glu** **tNAA**

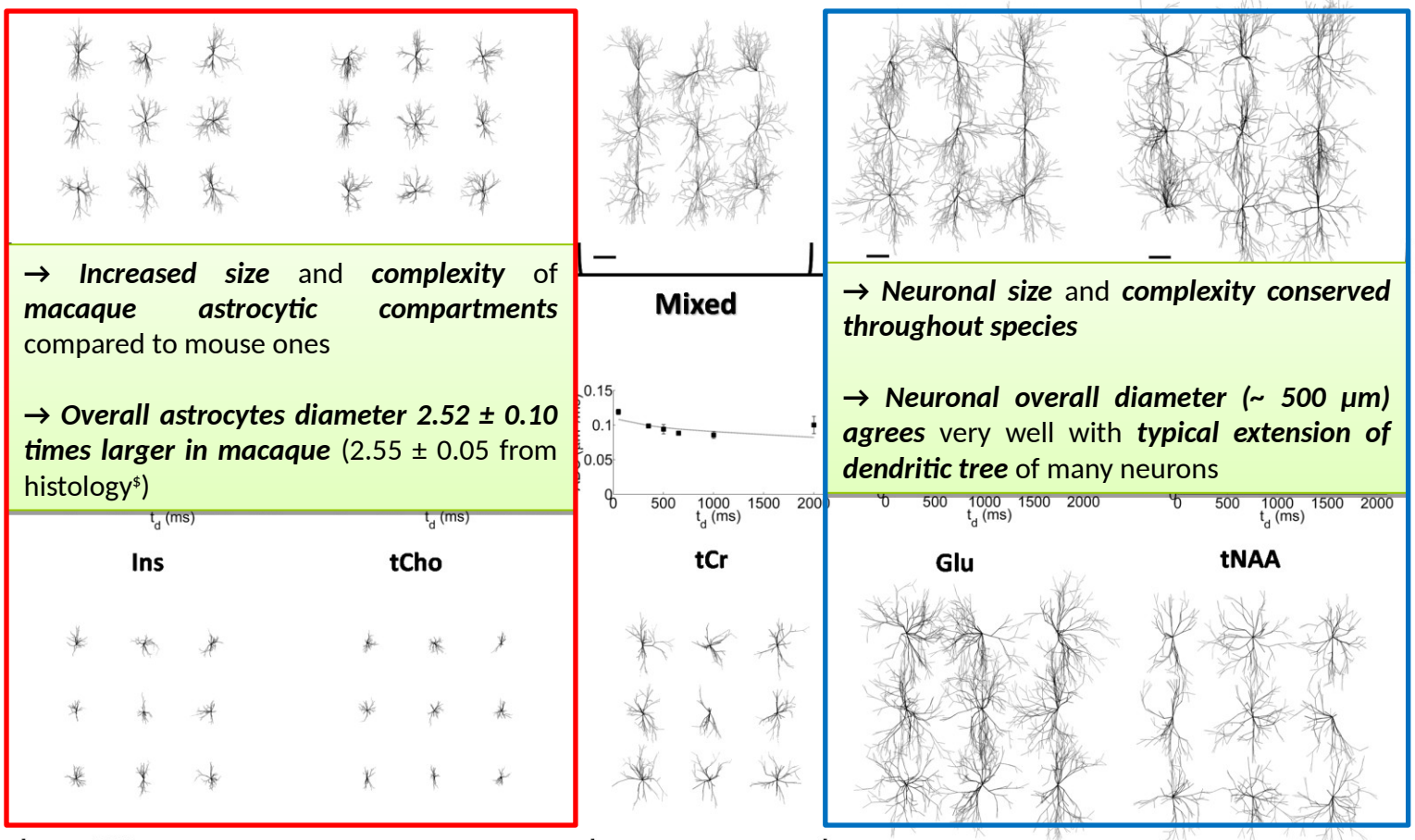

→ ***Increased size*** and ***complexity*** of ***macaque astrocytic compartments*** compared to mouse ones

→ ***Overall astrocytes diameter 2.52 ± 0.10 times larger in macaque*** (2.55 ± 0.05 from histology[$])

→ ***Neuronal size*** and ***complexity conserved throughout species***

→ ***Neuronal overall diameter (~ 500 µm) agrees*** very well with ***typical extension of dendritic tree*** of many neurons

Ins **tCho** **tCr** **Glu** **tNAA**

— 200 µm

Astrocytes **Mixed** **Neurons**

($) Oberheim N.A. et al. *Journal of Neuroscience* (2009) **29(10)**: 3276-3287

RESULTS

RECONSTRUCTED ASTROCYTES AND COMPARISON WITH HISTOLOGY

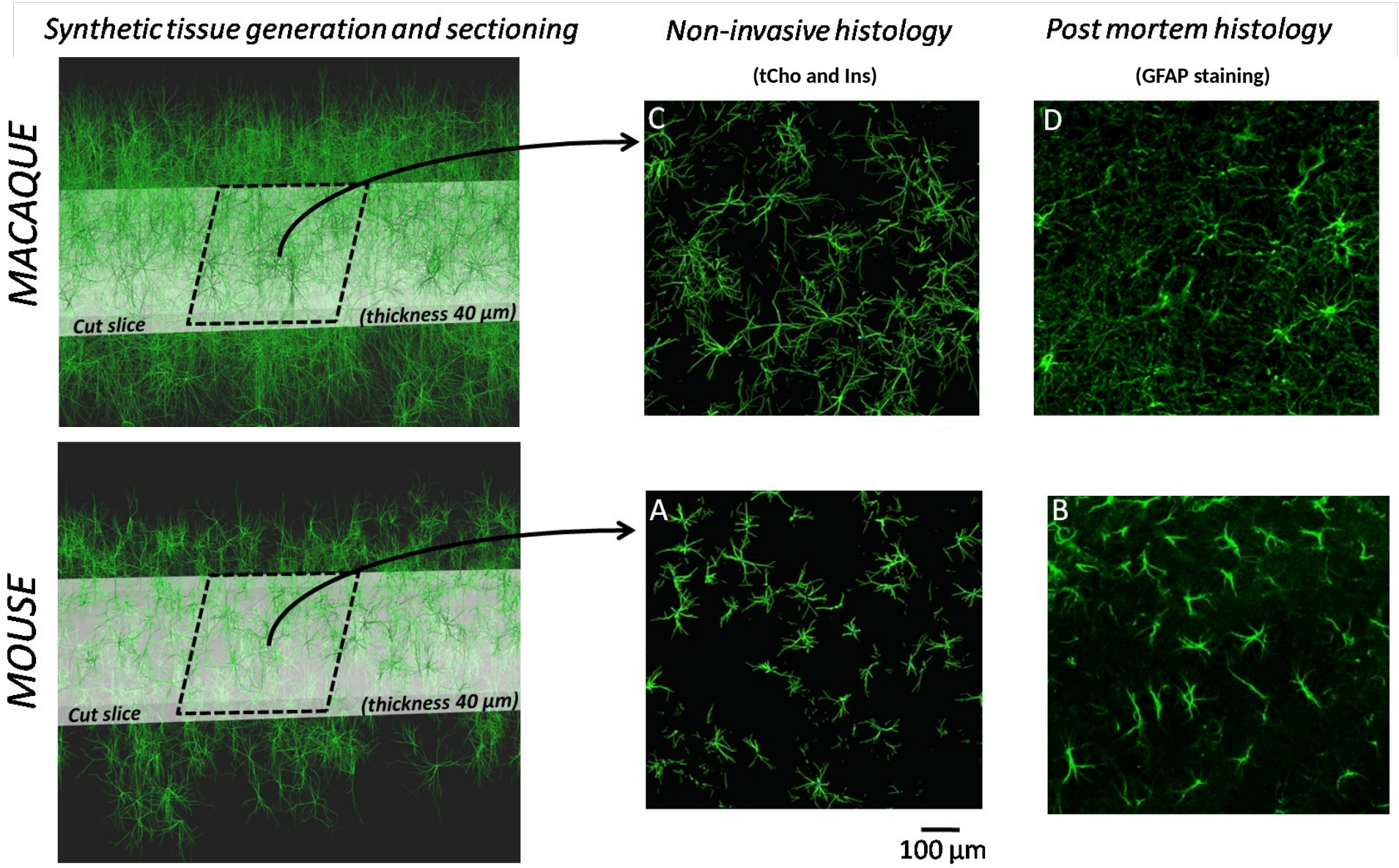

Palombo M. et al. *PNAS* (2016); **113**(*24*), 6671-6676

RESULTS

RECONSTRUCTED ASTROCYTES AND COMPARISON WITH HISTOLOGY

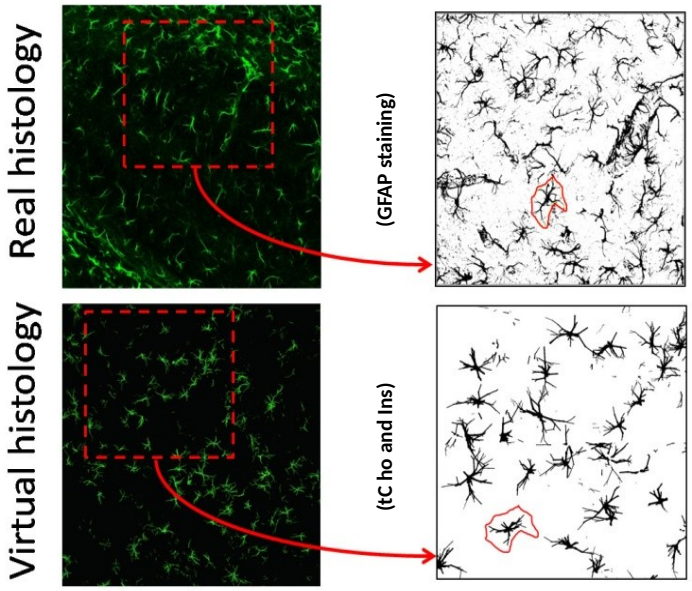

A) Zoom and binarization of bitmap images

→ ***Reasonable values for cell morphology parameters*** in both mouse and macaque brain

→ ***Good match between Sholl based metrics*** measured by real and virtual histology

High b-value DW-MRS signal simulations from realistic dendritic geometries

Basic cell-graph model

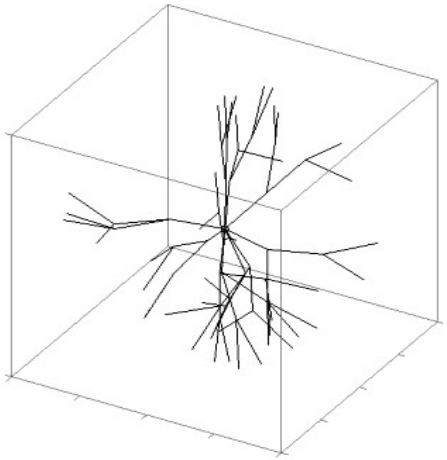

1) Presence of very long processes/axons;

2) Presence of leaflets/spines;

3) Presence of vericosities.

High b-value DW-MRS signal simulations from realistic dendritic geometries

Basic cell-graph model

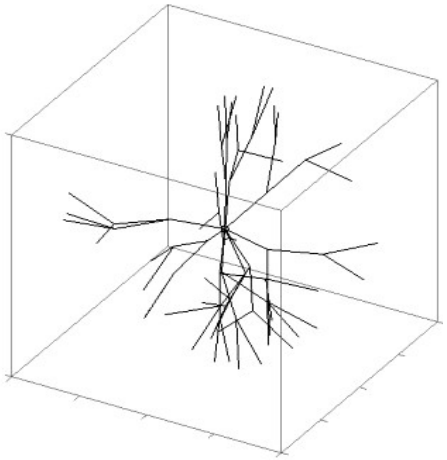

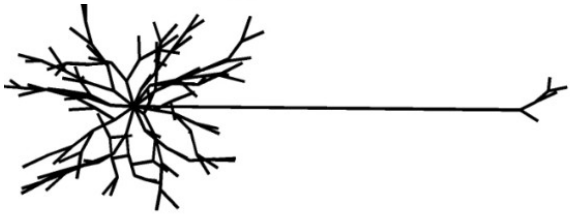

1) Presence of very long processes/axons;

2) Presence of leaflets/spines;

3) Presence of vericosities.

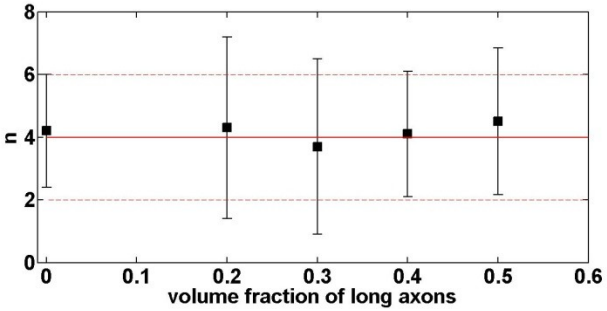

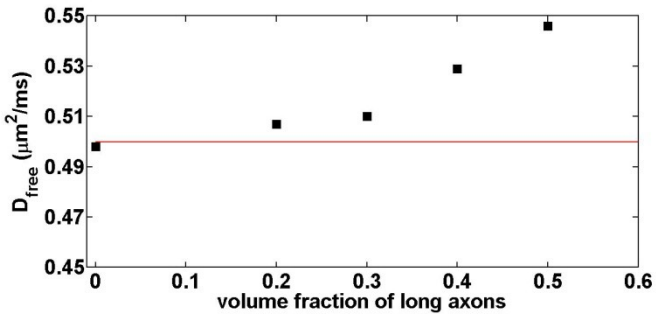

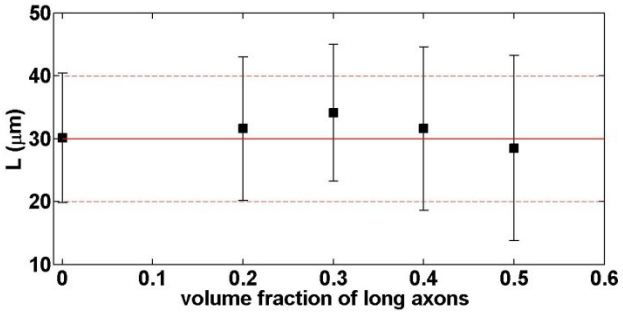

High b-value DW-MRS signal simulations from realistic dendritic geometries

Basic cell-graph model

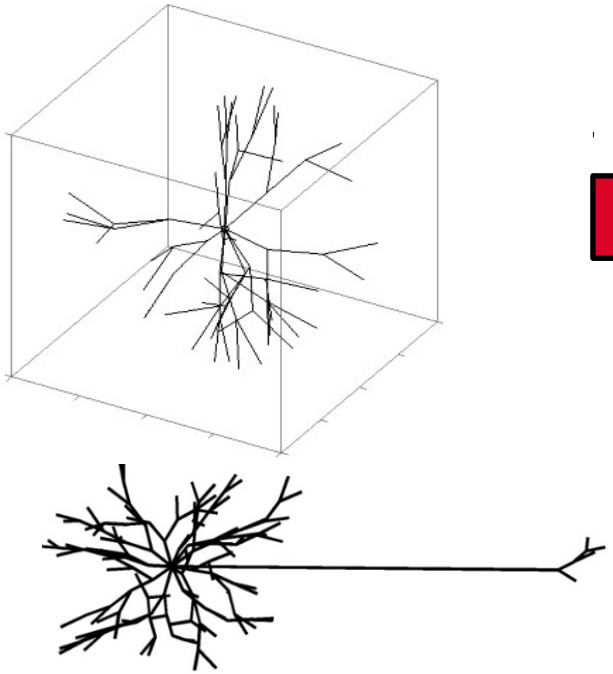

1) Presence of very long processes/axons;

2) Presence of leaflets/spines;

3) Presence of vericosities.

► It affects the estimation of D_{free} only, inducing overestimation of it.

High b-value DW-MRS signal simulations from realistic dendritic geometries

Basic cell-graph model

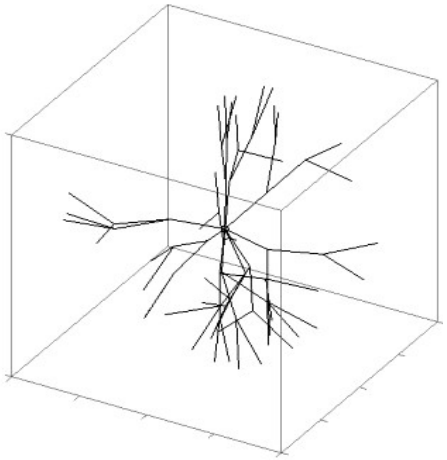

1) Presence of very long processes/axons;

2) Presence of leaflets/spines;

3) Presence of varicosities.

High b-value DW-MRS signal simulations from realistic dendritic geometries

Basic cell-graph model

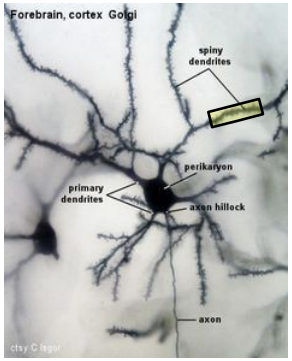

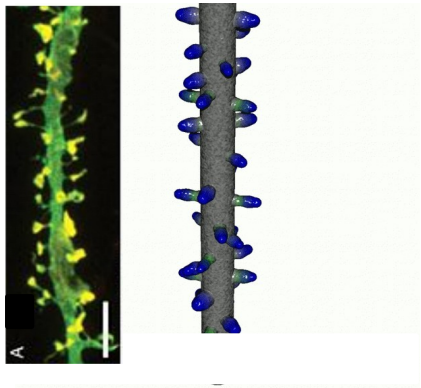

Real Simulated

1) Presence of very long processes/axons;

2) Presence of leaflets/spines;

3) Presence of varicosities.

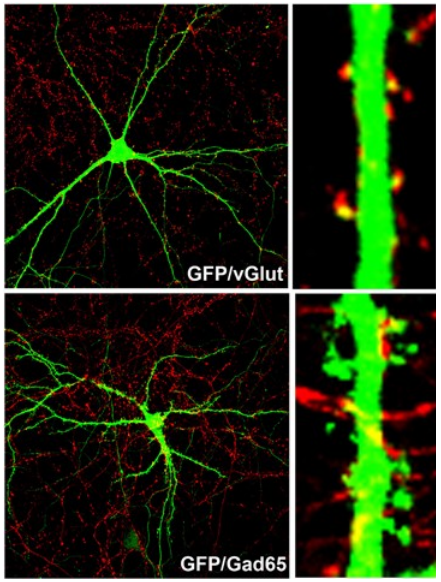

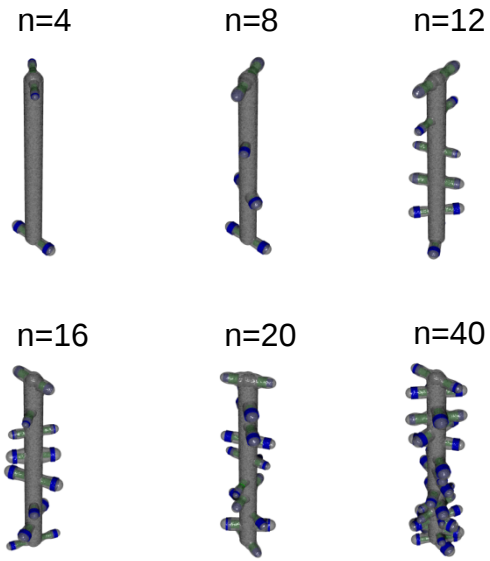

High b-value DW-MRS signal simulations from realistic dendritic geometries

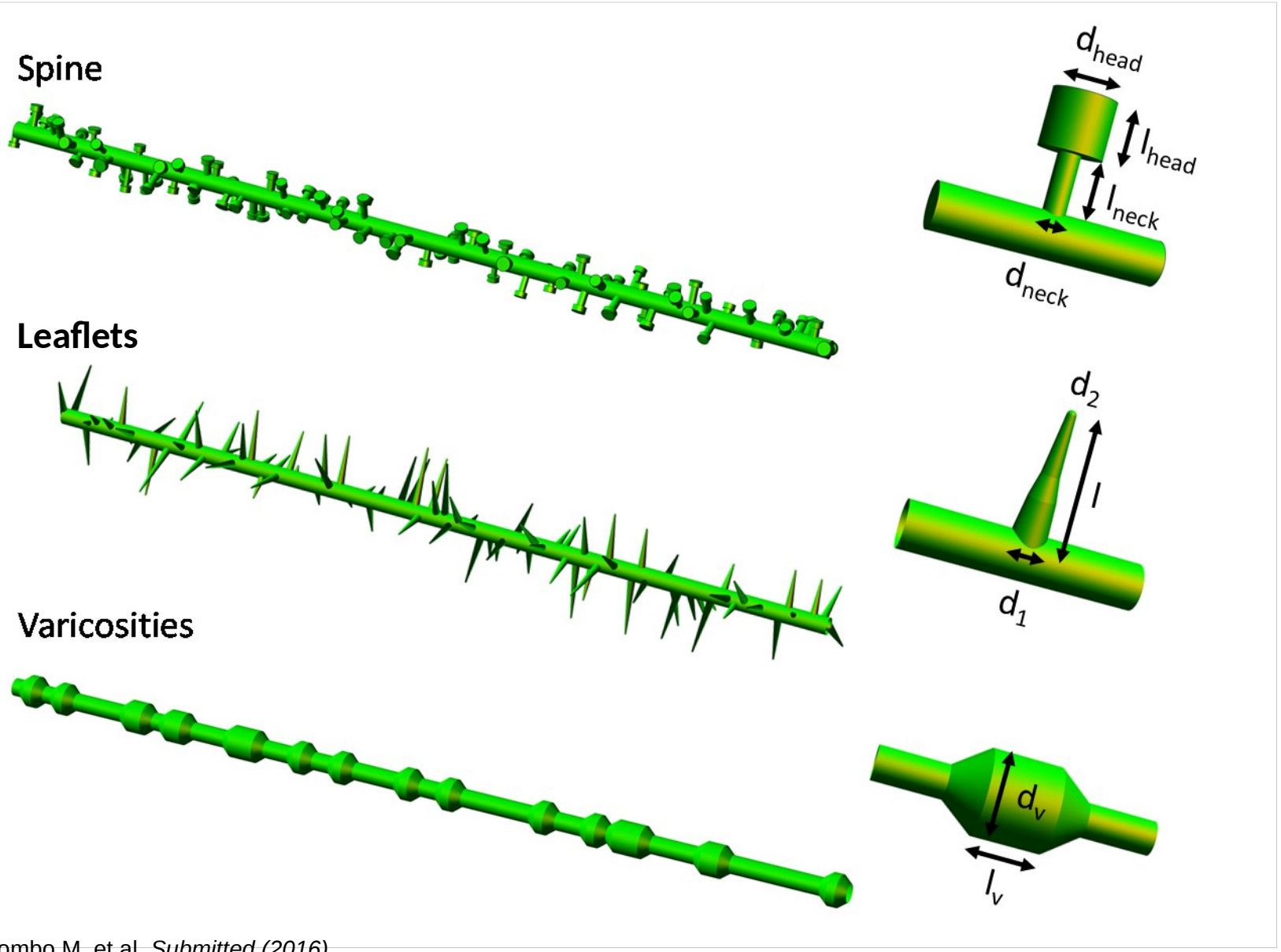

Palombo M. et al. *Submitted (2016)*

High b-value DW-MRS signal simulations from realistic dendritic geometries

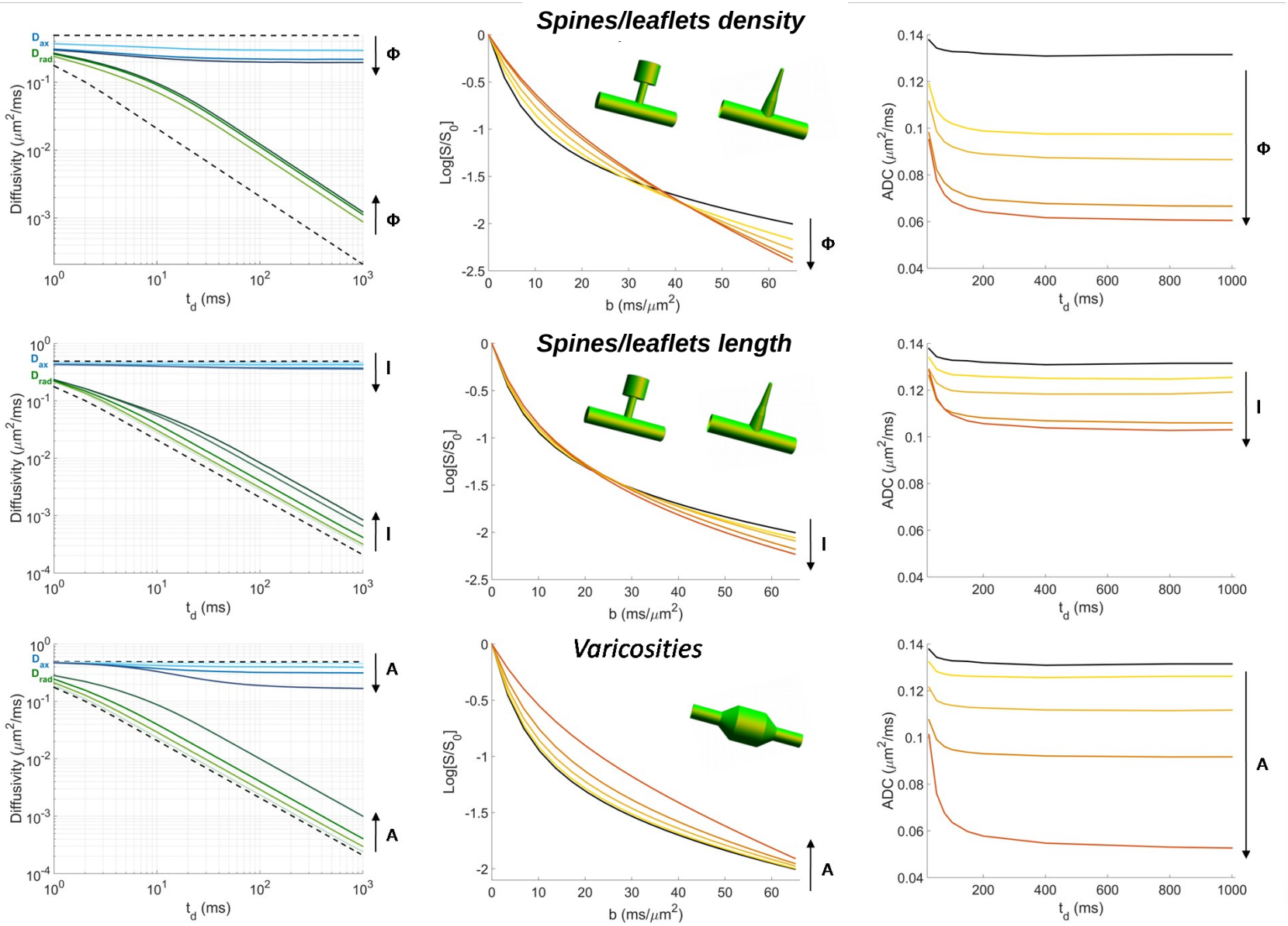

Palombo M. et al. *Submitted (2016)*

High b-value DW-MRS signal simulations from realistic dendritic geometries

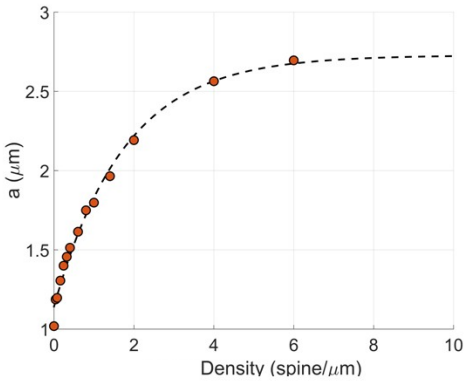

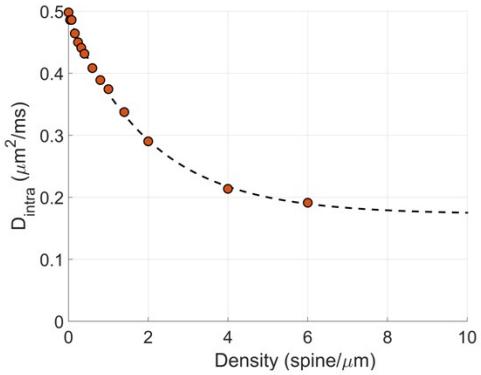

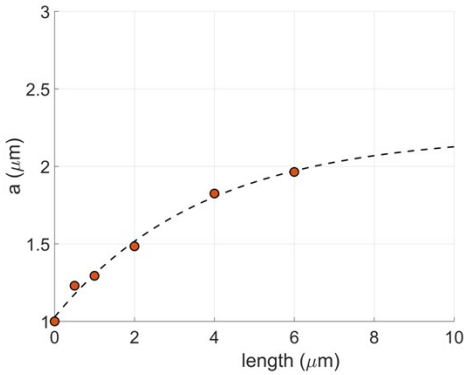

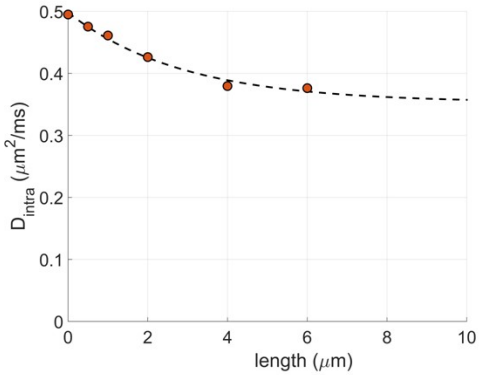

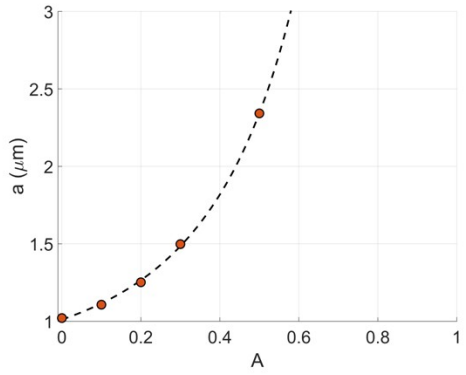

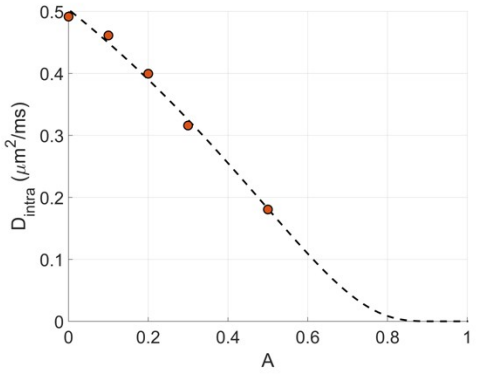

Spines/leaflets density

$$\frac{D_{intra}^{eff}}{D_0} = (2.4\phi^{0.35})^{-1.3} + [1 - (2.4\phi^{0.35})^{-1.3}]e^{-\phi}$$

$$r^{eff} = r_0 + 1.7(1 - e^{-0.6\phi})$$

Spines/leaflets length

$$\frac{D_{intra}^{eff}}{D_0} = [1.1(0.85l)^{0.065}]^{-1.4} + \left[1 - [1.1(0.85l)^{0.065}]^{-1.4}\right]e^{-0.85l}$$

$$r^{eff} = r_0 + 1.2(1 - e^{-0.25l})$$

Varicosities size

$$\frac{D_{intra}^{eff}}{D_0} = e^{-\frac{A}{1-A}}$$

$$r^{eff} = r_0 e^{0.86\frac{A}{1-A}}$$

Palombo M. et al. *Submitted (2016)*

High b-value DW-MRS signal simulations from realistic dendritic geometries

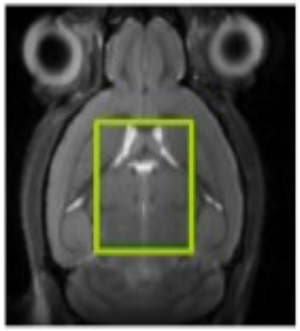

Metabolite	D_{intra}^{cyl} (µm²/ms)	a (µm)
NAA	0.339	0.62
Glutamate	0.440	0.90
Creatine	0.375	1.59
Taurine	0.436	1.30
Choline	0.308	1.33
Myo-Inositol	0.325	1.67

Neurons (D_0 from ultra short t_d)

NAA: Φ = 0.19 spine/µm; R_0 = 0.45 µm; l = 0.95 µm (D_0 = 0.454 µm²/ms)
Glu: Φ = 0.23 spine/µm; R_0 = 0.52 µm; l = 1.05 µm (D_0 = 0.476 µm²/ms)

From histology: Φ < 0.50 spine/µm; R_0 ~ 0.50 µm; l ~ 1.00 µm

Astrocytes (D_0 from ultra short t_d)

tCho: Φ = 0.70 leaflets/µm; R_0 = 0.75 µm; l = 2.65 µm (D_0 = 0.370 µm²/ms)
Ins: Φ = 0.73 leaflets/µm; R_0 = 1.07 µm; l = 2.79 µm (D_0 = 0.393 µm²/ms)

From histology: Φ ~ 1.00 leaflets/µm; R_0 ~ 1.00 µm; l > 2.50 µm

Merging structural information from high b-values / long t_d

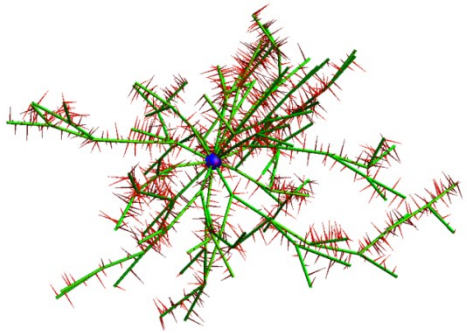

12 µm

Astrocyte and leaflets

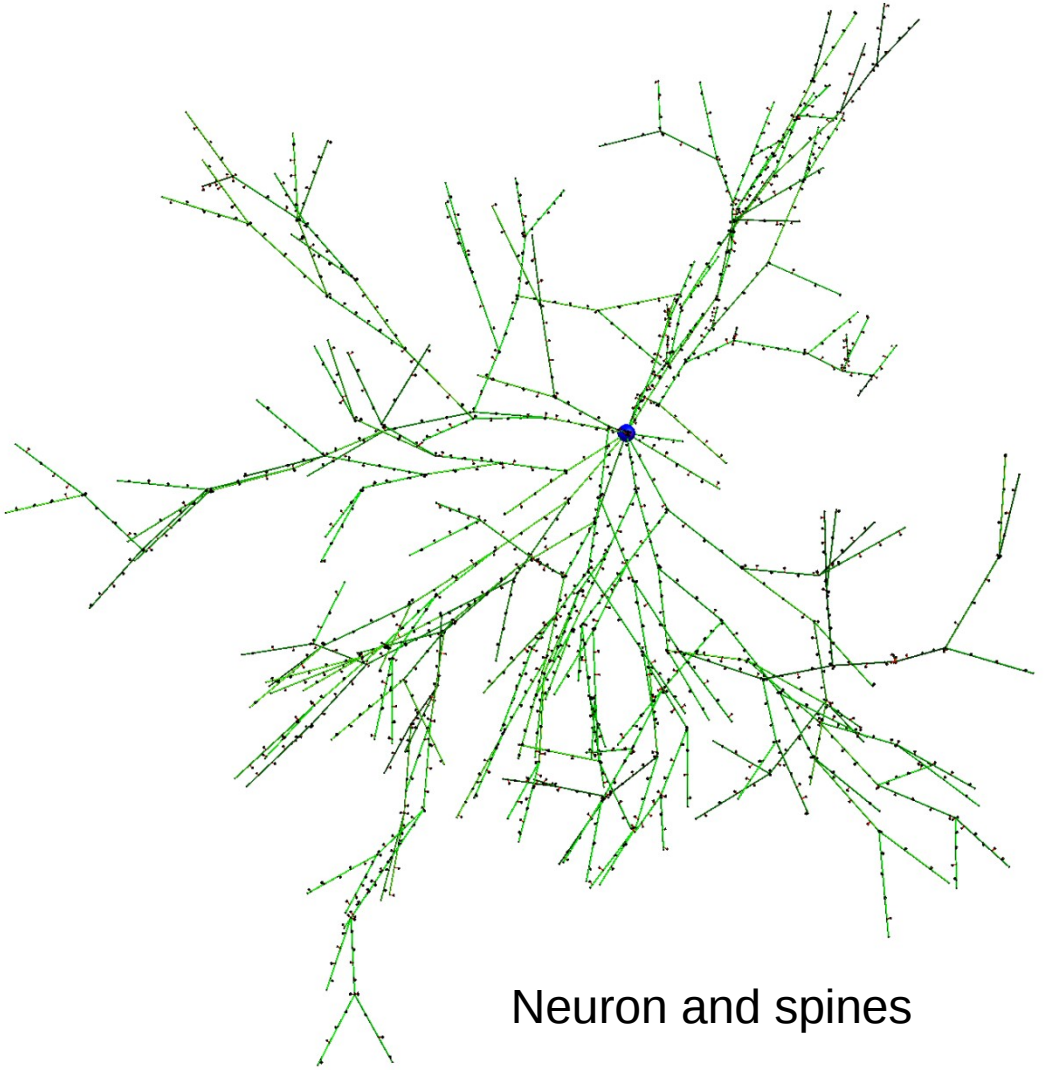

Neuron and spines

Merging structural information from high b-values / long t_d

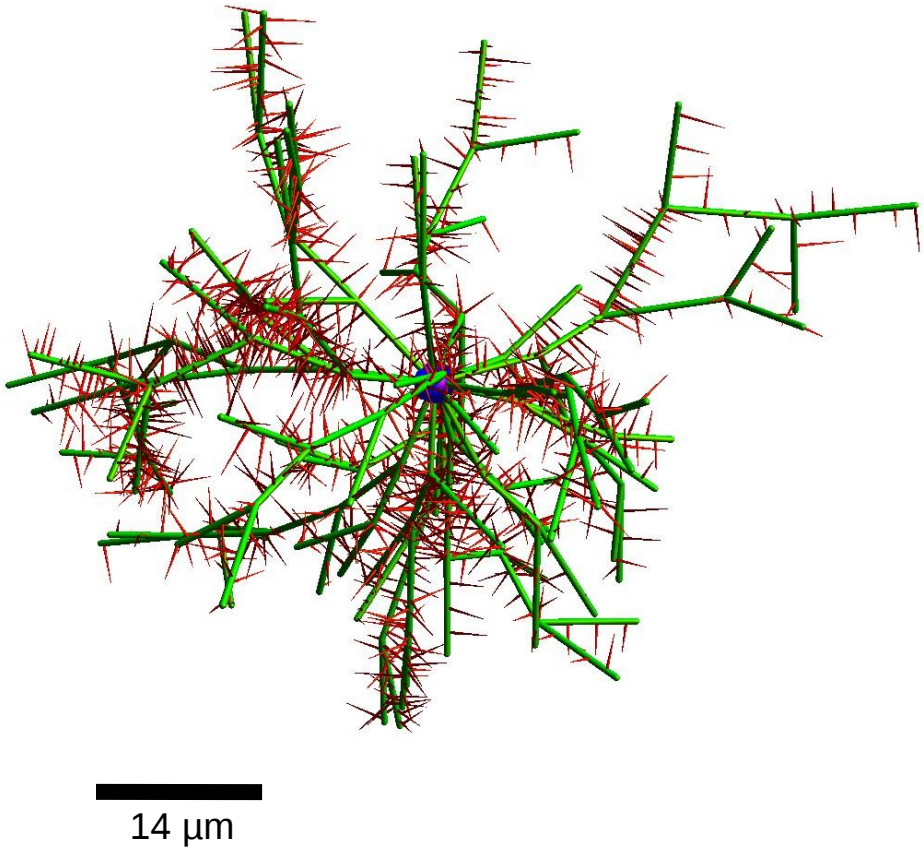

Virtual Astrocyte

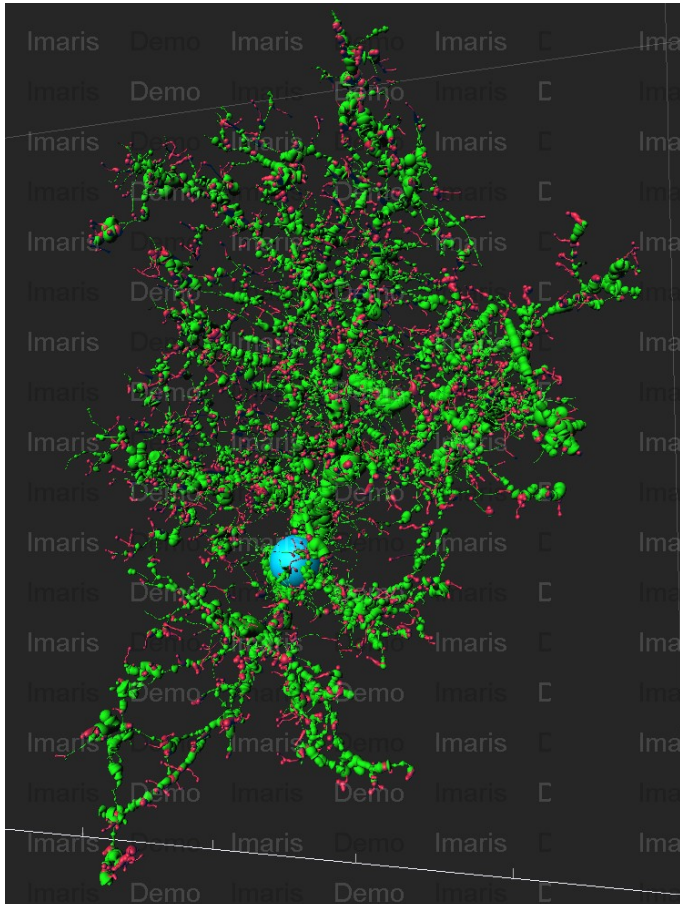

Real Astrocyte

Future perspectives in pathology applications

In CEA/MIRCen, Paris (France)

Injury and inflammation → Astrocytes reactivity

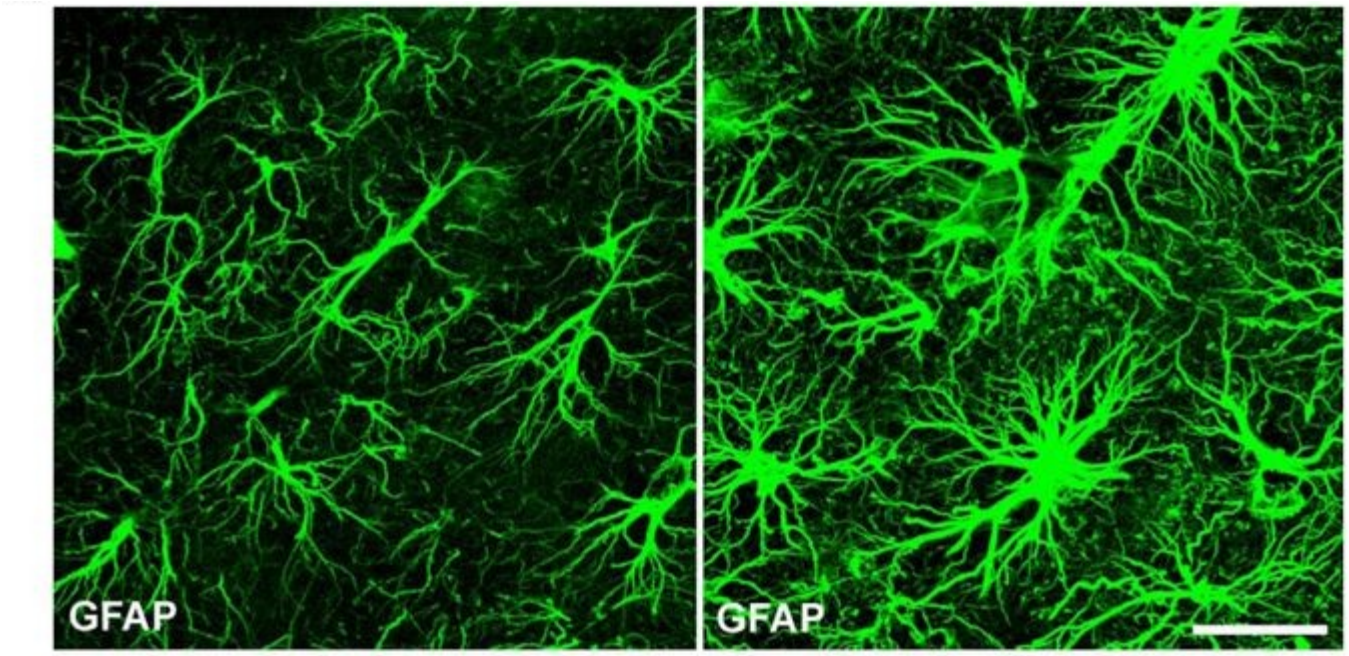

Astrocyte ‘Reactive’ Astrocyte

Future perspectives in pathology applications

In UCL, London (UK)

Simulate the whole brain → Cells growth and context aware interactions

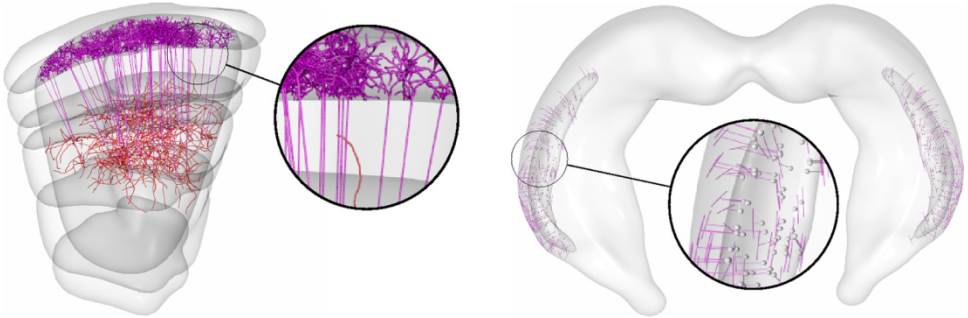

Vanherpe L., et al. *PRE (2016);* **94**, 023315

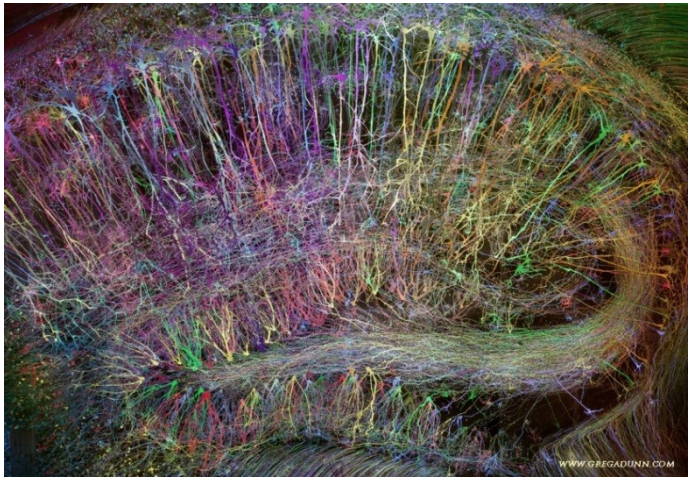

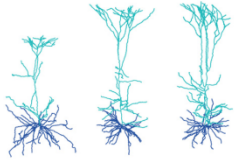

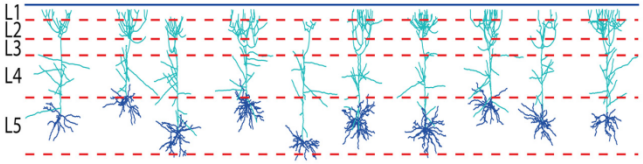

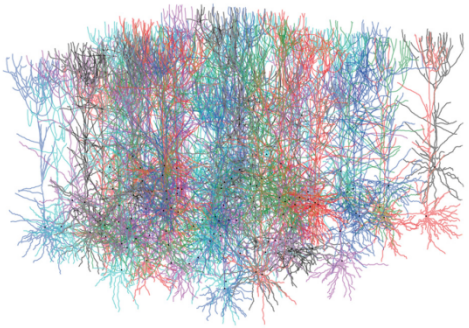

Torben-Nielsen B., et al. *Front. NeuroAnatomy (2014);* **8**, 92

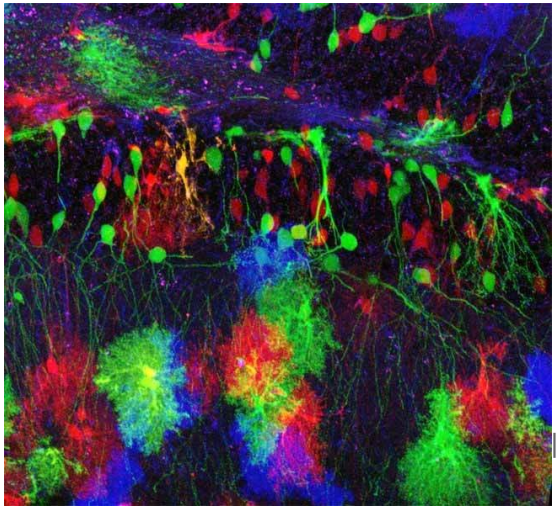

ACKNOWLEDGEMENTS

MIRCEN
MOLECULAR IMAGING RESEARCH CENTER

THANK YOU ALL FOR YOUR KIND ATTENTION!!!

erc

***INCELL* project**
(2013-2018)

ACKNOWLEDGEMENTS

THANK YOU ALL FOR YOUR KIND ATTENTION!!!

Contacts:

mrc.palombo@gmail.com

Commissariat à l'énergie atomique et aux énergies alternatives
MIRCen | 92260 Fontenay-aux-Roses
T. +33 (0)1 46 54 70 80 | F. +33 (0)1 46 54 70 80

Etablissement public à caractère industriel et commercial | RCS Paris B 775 685 019

Direction
Département
Service

RESULTS

EFFECTS OF MORPHOMETRIC PARAMETERS ON ADC TIME DEPENDENCE

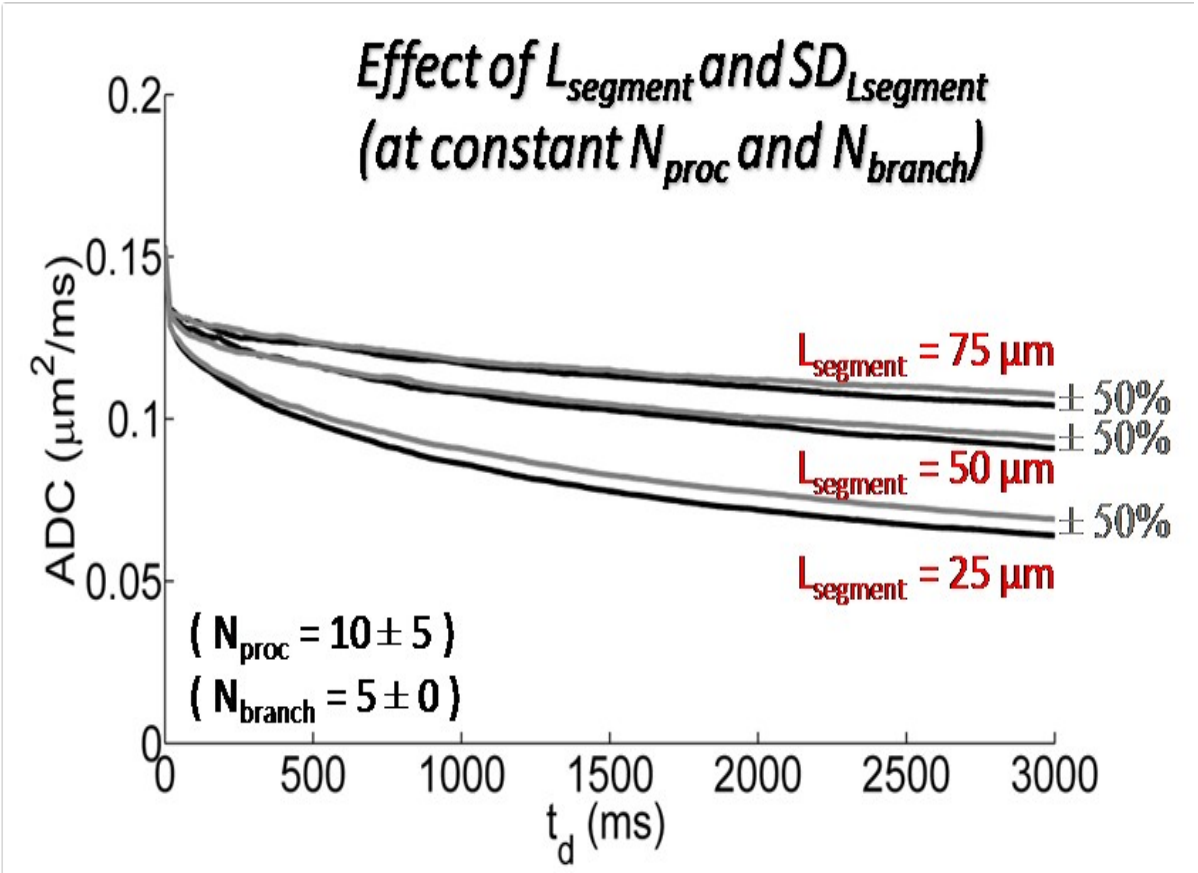

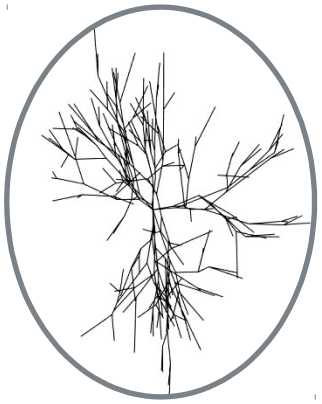

$L_{segment}$ = 75 µm

$L_{segment}$ = 50 µm

$L_{segment}$ = 25 µm

→ While ***$L_{segment}$*** has a ***strong effect***, the ***$SD_{Lsegment}$*** has a ***significant impact at long diffusion times only***.

Similar impact was found for N_{branch} and $SD_{Nbranch}$

RESULTS

EFFECTS OF MORPHOMETRIC PARAMETERS ON ADC TIME DEPENDENCE

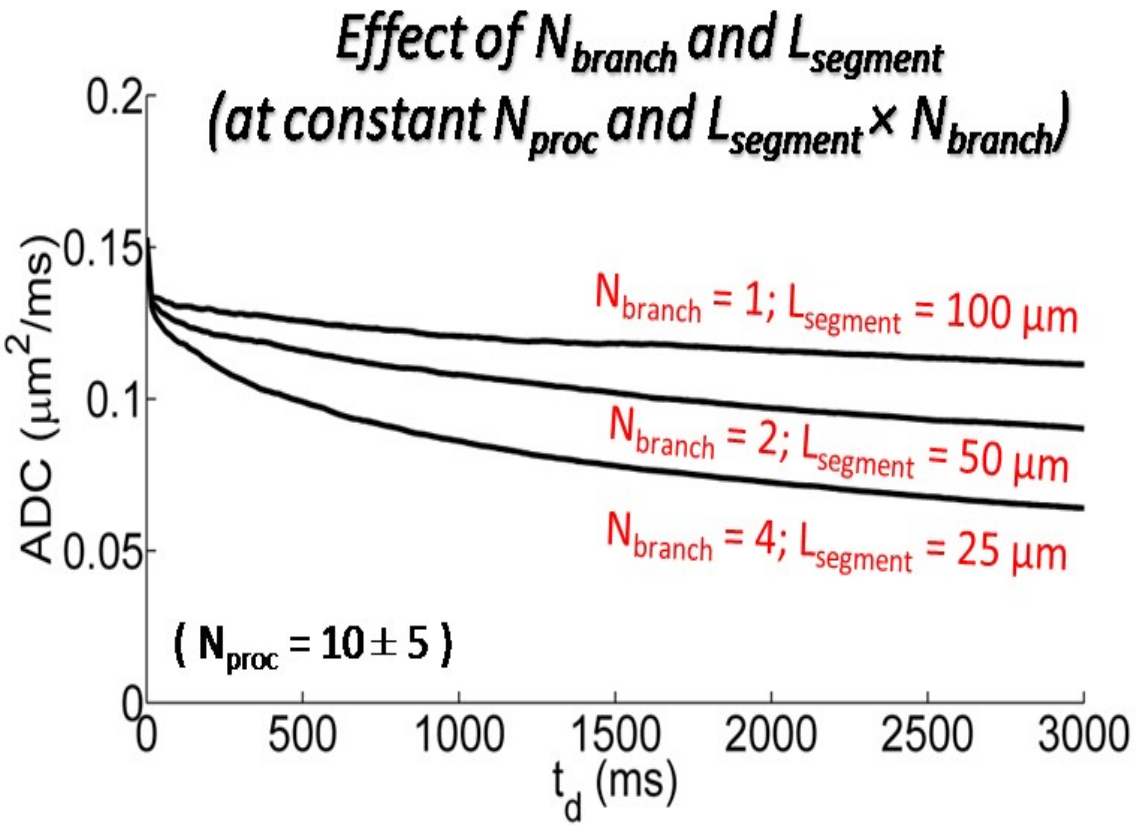

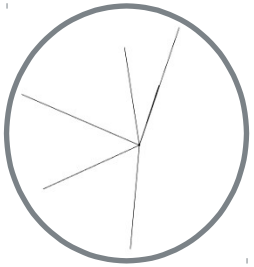

N_{branch} = 1; $L_{segment}$ = 100 µm

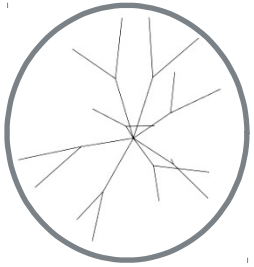

N_{branch} = 2; $L_{segment}$ = 50 µm

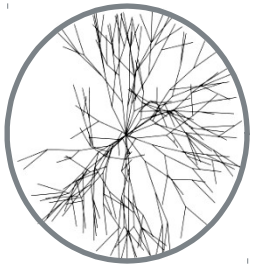

N_{branch} = 4; $L_{segment}$ = 25 µm

→ ***ADC*** time dependency ***does not only depend on*** total process length (***N_{branch} x $L_{segment}$***), ***but specifically depends on $L_{segment}$ and N_{branch}.***

HIGH G EXPERIMENTS AND MODELING

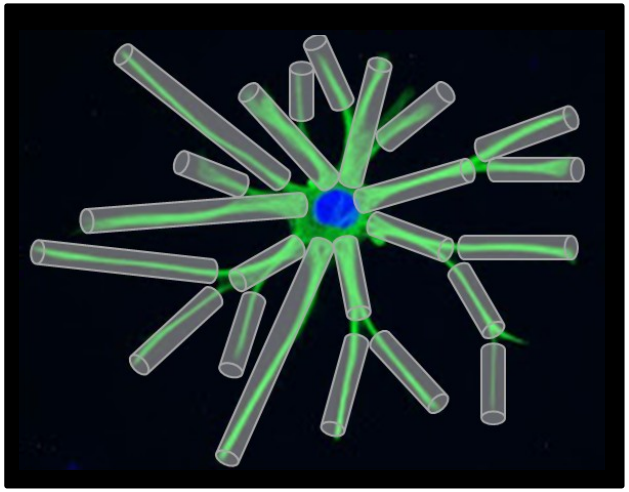

Strong g (short t_d)

✕ Segments length

✕ Number of consecutive bifurcation

→ Segments Diameter

HIGH G EXPERIMENTS AND MODELING

RESULTS

A

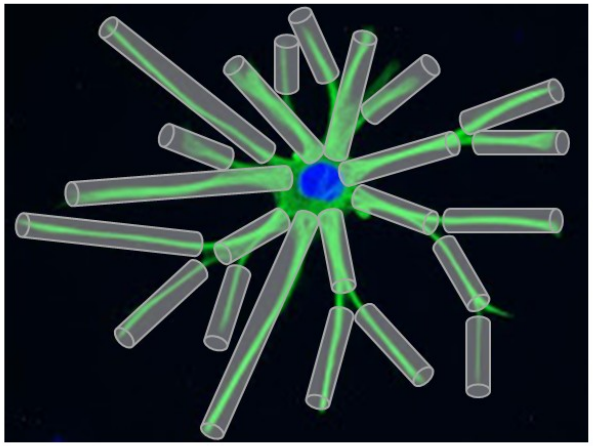

Randomly Oriented Cylinders Model

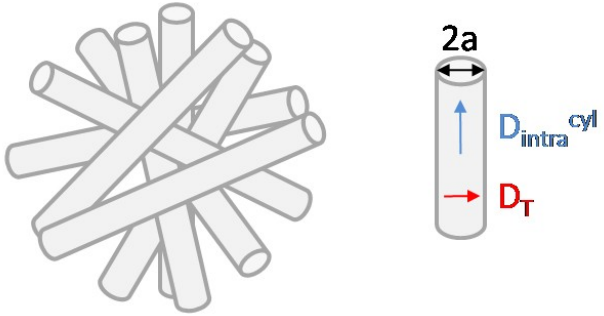

$$E_{cyl}(q,\Delta) = \exp(-D_T q^2 \Delta) \sqrt{\frac{\pi}{4q^2\Delta(D_{intra}^{cyl} - D_T)}}\ \mathrm{erf}\left[\sqrt{q^2\Delta(D_{intra}^{cyl} - D_T)}\right]$$

$$D_T = \frac{a^2}{4\Delta}\left[1 - \exp\left(-\frac{4D_{intra}^{cyl}\Delta}{a^2}\right)\right]$$

B

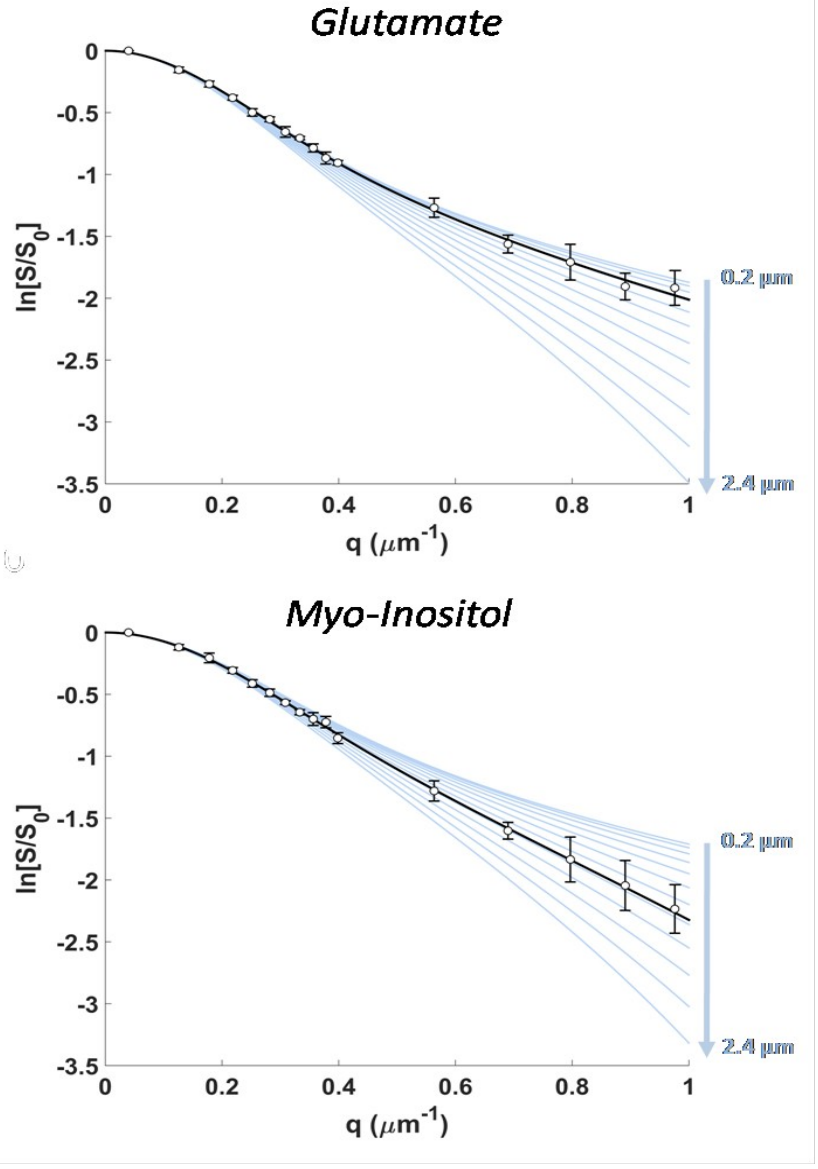

HIGH G EXPERIMENTS AND MODELING

RESULTS

A

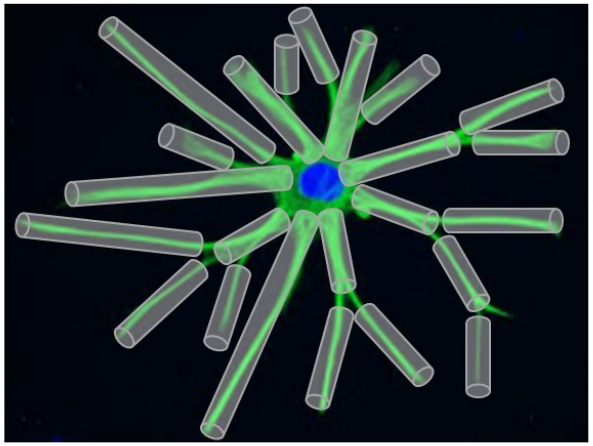

Randomly Oriented Cylinders Model

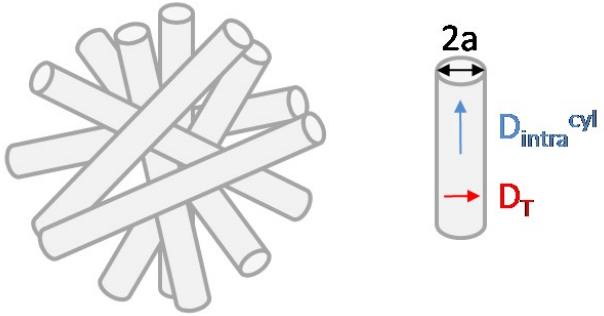

$$E_{cyl}(q,\Delta) = \exp(-D_T q^2 \Delta) \sqrt{\frac{\pi}{4q^2\Delta(D_{intra}^{cyl} - D_T)}}\ \mathrm{erf}\left[\sqrt{q^2\Delta(D_{intra}^{cyl} - D_T)}\right]$$

$$D_T = \frac{a^2}{4\Delta}\left[1 - \exp\left(-\frac{4D_{intra}^{cyl}\Delta}{a^2}\right)\right]$$

B

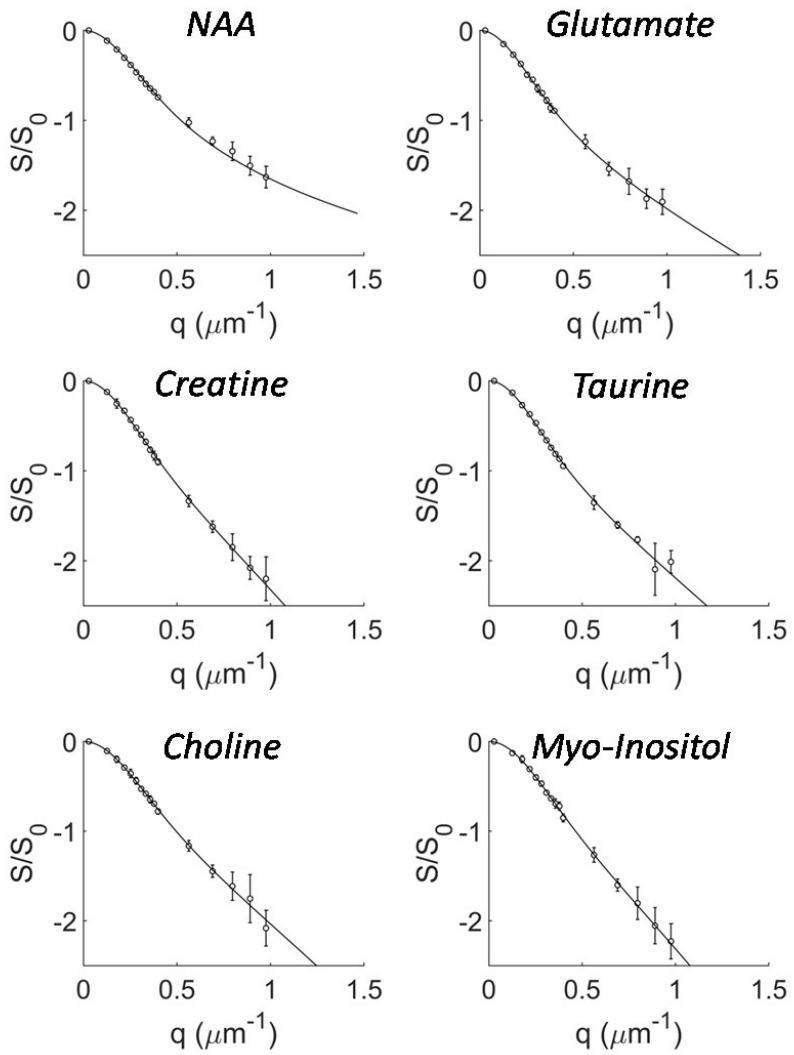

HIGH G EXPERIMENTS AND MODELING

RESULTS

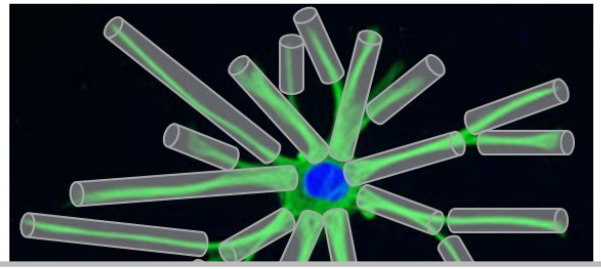

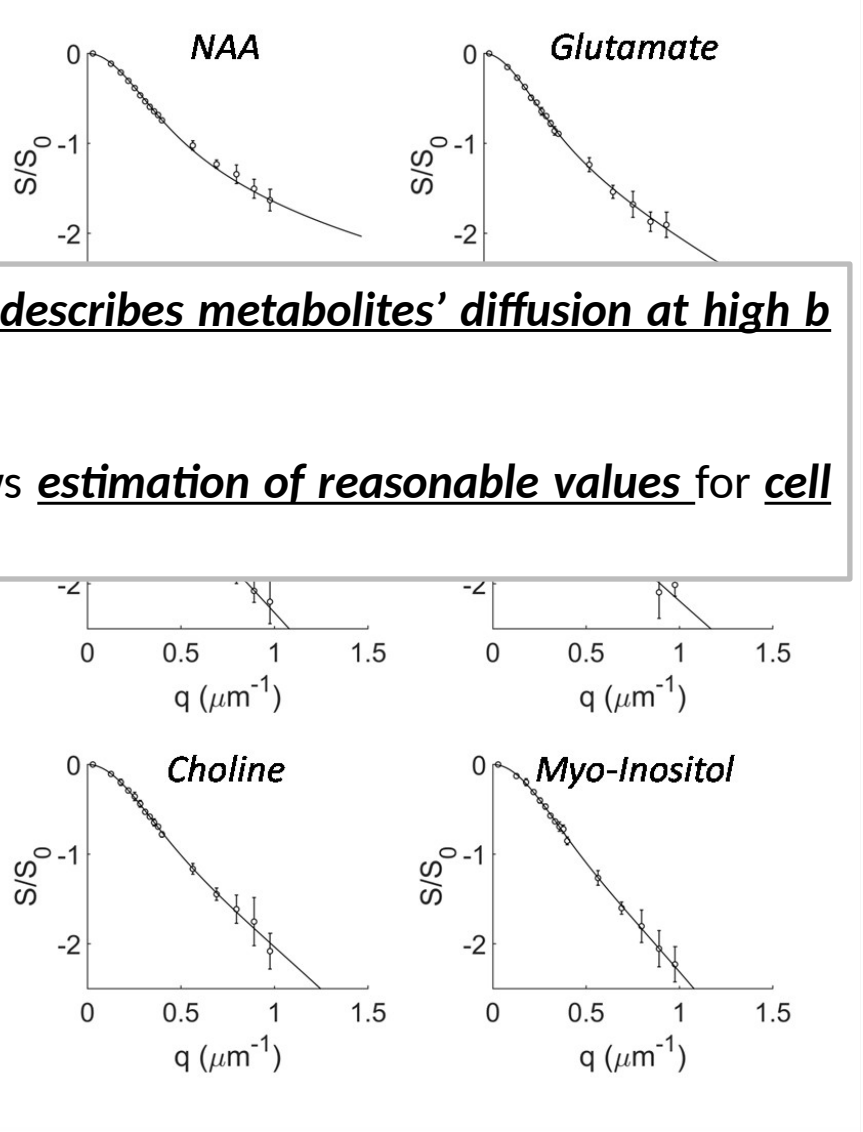

→ Randomly oriented cylinders model ***well describes metabolites' diffusion at high b values***

→ Randomly oriented cylinders model allows ***estimation of reasonable values*** for ***cell processes diameter***

Metabolite	D_{intra}^{cyl} (μm²/ms)	a (μm)
NAA	0.339	0.00
Glutamate	0.440	0.90
Creatine	0.375	1.59
Taurine	0.436	1.30
Choline	0.308	1.33
Myo-Inositol	0.325	1.67

HIGH G EXPERIMENTS AND MODELING

RESULTS

A

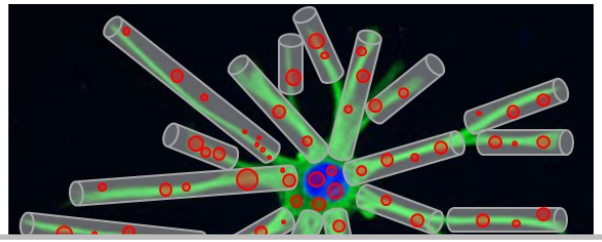

B

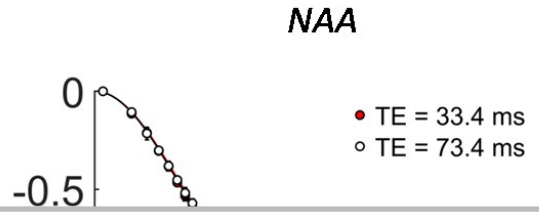

→ Modified randomly oriented cylinders model ***well describes NAA diffusion at high b values,*** allowing ***estimation of reasonable values*** for ***cell processes diameter and small compartments size.***

Spheres Model

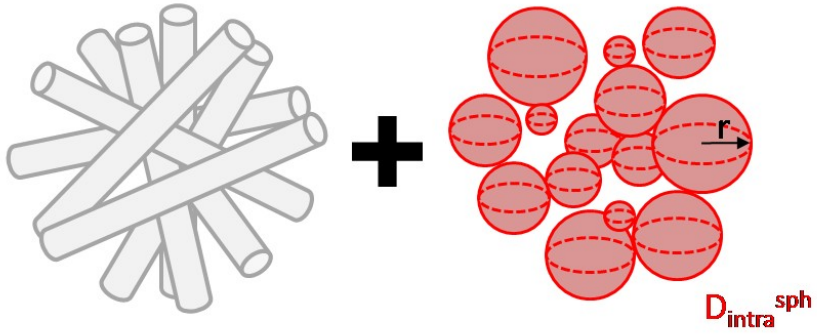

$$E_{tot}(q,\Delta) = v_{sph}\frac{\int_0^{\infty} r^3 P(r) E_{sph}(q,\Delta)\,dr}{\int_0^{\infty} r^3 P(r)\,dr} + (1 - v_{sph})E_{cyl}(q,\Delta)$$

q (μm^{-1})

C

Randomly Oriented Cylinders Model		
Metabolite	D_{intra}^{cyl} ($\mu m^2/ms$)	a (μm)
NAA (TE=73.4 ms)	0.335	0.62

Randomly Oriented Cylinders + Polydispersed Spheres Model				
Metabolite	D_{intra}^{sph} ($\mu m^2/ms$)	μ (μm)	σ (μm)	v_{sph} (%)
NAA (TE=33.4 ms)	0.168	0.019	0.028	2.0